



Development of venetoclax with 2-hydroxypropyl-beta-cyclodextrin inclusion complex for improved bioavailability

Smalant Kishor Patil, Padakanti Sandeep Chary, Sarvan Maddipatla, Y.V Madhavi, Siva Singothu, Vasundhra Bhandari, Ekta Pardhi, Kuldeep Kumar Bansal & Neelesh Kumar Mehra

To cite this article: Smalant Kishor Patil, Padakanti Sandeep Chary, Sarvan Maddipatla, Y.V Madhavi, Siva Singothu, Vasundhra Bhandari, Ekta Pardhi, Kuldeep Kumar Bansal & Neelesh Kumar Mehra (21 Jan 2024): Development of venetoclax with 2-hydroxypropyl-beta-cyclodextrin inclusion complex for improved bioavailability, Journal of Biomolecular Structure and Dynamics, DOI: [10.1080/07391102.2024.2305695](https://doi.org/10.1080/07391102.2024.2305695)

To link to this article: <https://doi.org/10.1080/07391102.2024.2305695>



[View supplementary material](#)



Published online: 21 Jan 2024.



[Submit your article to this journal](#)



Article views: 165



[View related articles](#)



[View Crossmark data](#)



Citing articles: 1 [View citing articles](#)



Development of venetoclax with 2-hydroxypropyl-beta-cyclodextrin inclusion complex for improved bioavailability

Smalant Kishor Patil^{a*}, Padakanti Sandeep Chary^{a*}, Sarvan Maddipatla^b, Y.V Madhavi^b, Siva Singothu^c, Vasundhra Bhandari^c, Ekta Pardi^a, Kuldeep Kumar Bansal^d and Neelesh Kumar Mehra^a

^aPharmaceutical Nanotechnology Research Laboratory, Department of Pharmaceutics, National Institute of Pharmaceutical Education and Research (NIPER), Hyderabad, Telangana, India; ^bDepartment of Chemical Sciences, National Institute of Pharmaceutical Education and Research (NIPER), Hyderabad, Telangana, India; ^cDepartment of Pharmacoinformatics, National Institute of Pharmaceutical Education and Research (NIPER), Hyderabad, Telangana, India; ^dPharmaceutical Sciences Laboratory, Faculty of Science and Engineering, Åbo Akademi University, Turku, Finland

Communicated by Ramaswamy H. Sarma

ABSTRACT

Cyclodextrin complexes loaded with venetoclax for improved solubility and therapeutic efficacy as repurposed drug. The venetoclax-cyclodextrin inclusion complex was prepared using kneading method. Primarily in-silico molecular docking study was performed to examine the possible interaction between venetoclax and hydroxypropyl-β-cyclodextrin (HP-β-CD) and extensively characterized. The in-vitro studies were performed using A-549 lung epithelial cancer cells. The in-vivo pharmaco-kinetic studies was performed on wistar rats. The aqueous solubility of venetoclax was increased upto 3.16 folds, as compared with pure venetoclax with entrapment efficiency (EE%) was determined 95.44 ± 0.3%. In-vitro cytotoxicity studies were carried on A-549 lung epithelial cancer cells, wherein BCL-2 receptors were highly over-expressed and IC 50 values for venetoclax and venetoclax- HP-β-CD complex was calculated at 24 and 48 hrs in the order of 1.241 μg/ml, 0.68 μg/ml and 0.757719 μg/ml, 0.6125 μg/mL, respectively. The oral bioavailability was increased 4.03 times compared to the pure drug. The venetoclax-HP-β-CD inclusion complexes showed the increased aqueous solubility with improved anticancer activities.

Abbreviations: VEN: Venetoclax; HP-β-CD: Hydroxypropyl-beta-cyclodextrin; ACN: Acetonitrile; DMSO: Dimethyl sulfoxide; DCM: Dichloromethane; NaCl: Sodium chloride; DCC: Dicyclohexyl carbodiimide; Tween-80: Polysorbate 80; HCl: Hydrochloric acid; PDP: Potassium dihydrogen phosphate; NaOH: Sodium hydroxide; DMF: Dimethyl formamide; BCL-2: B-cell lymphoma-2; SEM: Scanning electron microscopy; DSC: Differential scanning calorimetry; NMR: Nuclear magnetic resonance; HPLC: High performance liquid chromatography

ARTICLE HISTORY

Received 8 July 2023
Accepted 9 January 2024

KEYWORDS

Cyclodextrin; lung epithelial; molecular modeling; caspase; MTT assay



1. Introduction

Cancer, a globally pervasive affliction, register approximately 18.1 million incident cases and claims 10 million lives annually. Predominant diagnosed cancers are breast (2.26 million), prostate (1.41 million), and lung (2.21 million) cancers (Ferlay et al., 2021). Established cancer risk factors include an unhealthy diet, alcohol consumption, genetic predisposition, tobacco use, lifestyle alterations, infections, obesity, and environmental factors triggering abnormal tumor development at specific sites (Avgerinos et al., 2019; Pavlidis et al., 2005).


The primary modalities for cancer management encompass surgery, chemo-radiation therapy (CRT), hematopoietic cell transplantation (HCT), and medical oncology. Surgery assumes a pivotal role in addressing head, mouth and oral cancer based on criteria such as depth of infiltration, bone

proximity, size and tumor location. CRT emerges as a primary therapeutic approach for advanced mouth, head and neck cancers, serving as adjuvant therapy for unfavorable clinical features. Various formulations, including carbon nanotubes, liposomes, niosomes, and nano-particles, offer diverse avenues in cancer treatment (Mehra et al., 2013, 2014; Palakurthi et al., 2017).

Several drugs, such as Abemaciclib, Doxorubicin, and paclitaxel, by the United States of Food & Drug administration (USFDA), exhibit drawbacks like high dosage, low bio-availability and side effects (Yang et al., 2002). Addressing these challenges, novel drug delivery systems aim to develop dosage forms with selective drug targeting. The BCL-2 inhibitor Venetoclax (VEN) stands out for treating Chronic Lymphatic Leukemia's (CLL's) (Anderson et al., 2016; Deeks, 2016) and Acute Myeloid Leukemia's (AML's). However, VEN

CONTACT Neelesh Kumar Mehra  neesh@niperhyd.ac.in, neesh81mph@gmail.com  Pharmaceutical Nanotechnology Research Laboratory, Department of Pharmaceutics, Ministry of Chemical and Family Welfare, National Institute of Pharmaceutical Education and Research (NIPER), Hyderabad, Telangana 500 037, India.

*These authors contributed equally.

 Supplemental data for this article can be accessed online at <https://doi.org/10.1080/07391102.2024.2305695>.

© 2024 Informa UK Limited, trading as Taylor & Francis Group

faces hurdles like low aqueous solubility (0.000933 mg/ml) and bioavailability (5.4%). Overcoming these limitations involves incorporating of VEN into a suitable drug delivery system, enhancing aqueous solubility through cyclodextrin complexes (Alhoshani et al., 2020; Bhalani et al., 2022). Natural cyclodextrin includes (i) alpha cyclodextrin (α -CDs), (ii) beta cyclodextrin (β -CDs), and (iii) gamma cyclodextrin (γ -CDs) play a crucial role in inclusion complex development (de Miranda et al., 2011). Beta cyclodextrin, with its hydrophilic external covering and hydrophobic internal core, proves to encapsulating a wide range of guest molecules, thereby increasing drug solubility and enhancing permeation for macromolecular drugs. Gamma cyclodextrin, with its large cavity size and high aqueous solubility, faces challenges in membrane penetration and rapid digestion from circulatory systems (Goh et al., 2022; Palakurthi et al., 2017; Loftsson et al., 2005; Suvarna et al., 2017). Recent derivatives, such as di-methyl- β -cyclodextrin, sulfobutyl-ether- β -cyclodextrin, and hydroxy-propyl- β -cyclodextrin, have been introduced to address these challenges and enhances the aqueous solubility of poorly hydrophobic drugs (Charumanee et al., 2016; Pereira et al., 2021).

This research endeavors to incorporate the poorly aqueous soluble drugs in cyclodextrin cavities, enhancing solubility and therapeutic activity on A-549 lung epithelial cells. The BCL-2 API moiety aims to block and integrate with cell organelles in various cancer cells. The venetoclax-cyclodextrin complex undergoes design, development, physicochemical characterization, in silico molecular modeling, *in vitro* drug release, and cytotoxicity studies on A-549 lung epithelial cells.

2. Materials and methods

Venetoclax was obtained as gift sample from the Dr Reddy Pharmaceutical Pvt Ltd, Hyderabad. Hydroxypropyl- β -cyclodextrin (HP- β -CD) was purchased from Tokyo Chemicals Industry Co. Ltd. Hyderabad, India, Tween® 80 analytical grade was obtained from Avra Synthesis Pvt. Ltd. Hyderabad, India, acetonitrile HPLC grade were procured from Sysco's Research Laboratory Pvt. Ltd. New Mumbai, India. All others chemicals, such as dimethyl sulfoxide (DMSO), dichloromethane (DCM), had acquired from Sysco's Research Laboratory Pvt. Ltd. (New Mumbai, India). A-549 cell line was purchased from National Centre for Cell Sciences (NCCS) Pune, India. RPMI media, trypsin, fetal bovine serum, ethidium bromide, acridine orange, 3-(4,5-Dimethylthiazol-2-yl)-2,5-diphenyltetrazolium bromide, fluorescein isothiocyanate and 4'-6-diamino-2-phenylindoles had acquired from Thermo Fisher Scientific India Pvt. Ltd. Hyderabad and Hi-Media Pvt. Ltd, Mumbai, respectively. All the reagents, 0.22 μ m PTFE filter and solvents were used as received.

2.1. Stoichiometric determination

2.1.1. Phase solubility study

A comprehensive phase solubility investigation of venetoclax (VEN) in hydroxypropyl- β -cyclodextrin (HP- β -CD) was

executed employing the methodologies put forth by Cabral and Hadgraft in 1990, specifically the Higuchi and Connor approaches (Cabral & Hadgraft, 1990). Aqueous solution of HP- β -CD with varying concentrations (1.6215, 1, 0.1, 0.01, 0.001, 0.0001, 0.00001 mM) were meticulously prepared in an aqueous milieu. Excessive quantities of VEN were introduced into each solution and subjected for shaking (IKA, Germany) operating at 100 ± 5 rpm and maintained at 37 ± 0.5 °C for a duration of 72 hrs.

Upon achieving equilibrium, the samples underwent centrifugation (Eppendorf Minispin, Hamburg, Germany) at 10,000 rpm for 15 min. Subsequently, the supernatant was collected and subjected to filtration through a 0.45 μ m filter membrane (Sigma Aldrich, Hyderabad, India). Furthermore, dilutions were carried out for the respective samples, and these were quantified using the analytical HPLC method (Lodagekar et al., 2019). The phase solubility curve was plotted by correlating the concentration of VEN (expressed in micro-molar units) against the concentration of HP- β -CD. Simultaneously, the stability constant (K_c) was determined from the resulting graph by using the following equation:

$$K_c : 1 : 1 = \frac{\text{Slope}}{S_o(1 - \text{slope})}$$

whereas, S_o = intrinsic solubility of Venetoclax in water.

2.2. In silico studies

2.2.1. Molecular modelling

2.2.1.1. Ligand preparation. The Venetoclax structure was drawn and optimized with the help of a 2D sketcher of Schrodinger suite 20-3 as well as evaluated for docking by allocating the bond angles and orders utilizing Lig-Prep modules. The conversion of Venetoclax from 2D structure to 3D structure was done in the Lig-Prep module, as well as the energy was reduced utilizing OPLS4. By using the Epik module of Lig-Prep the ionizing state of Venetoclax was developed at a particular pH (7.0 ± 2.0) and kept remaining parameters to pre-determined values.

2.2.1.2. Excipient preparation. To perform molecular docking, the crystal structures of cyclodextrin glycosyl-transferase were collected from the protein data bank with PDB ID: 3CGT. The protein structure was prepared by the addition of hydrogens atoms, removal of water molecules beyond 5 Å of het state, creating disulfide bonds, and filling of missing loops in the protein using the protein preparation wizard module, Schrodinger 2022-4. Later, Optimization and energy minimization were done using PROKA at pH 7.4 and OPLS4 force field (Shukla et al., 2020). Furthermore, HP- β -CD was taken out from the protein to perform docking against venetoclax.

2.2.1.3. Grid generation and molecular docking. The binding site grid of HP- β -CDs had generated by choosing the centroid of the HP- β -CDs. GLIDE docking module from the Schrödinger Suite was utilized to carry out molecular docking of VEN with HP- β -CDs. Extra precisions (XP) docking

calculation were carried out, and the parameters of partial charge cut-off and scaling factor were set at the pre-determined values of 0.80 and 0.15, respectively (Rudrangi et al., 2015).

Molecular docking between prepared β -cyclodextrin and venetoclax was carried out using glide module in the extra precision mode. The docking score was calculated using the below mentioned equation; $\text{Glide Score} = E_{\text{coul}} + E_{\text{vdW}} + E_{\text{bind}} + E_{\text{penalty}}$.

2.2.1.4. Molecular mechanics-generalized Born surface area (MM-GBSA) assay. The binding free energies of the β -cyclodextrin-venetoclax inclusive complex were processed by the prime MM-GBSA module of Maestro 2022-1. This method determines each ligand's relative binding-free energy (ΔG_{bind}).

$$\Delta G_{\text{bind}} = \Delta G_{\text{(Solv)}} + \Delta E_{\text{(MM)}} + \Delta G_{\text{(SA)}}$$

where $\Delta G_{\text{(Solv)}}$ is the difference in GBSA solvation energy of the complex and the sum of the solvation energies for individuals; $\Delta E_{\text{(MM)}}$ is the difference in the minimized energies between complex and the sum of the energies of the individuals; and $\Delta G_{\text{(SA)}}$ is the difference in surface area energies of the complex and sum of the surface area energies for the individuals.

2.2.1.5. Molecular dynamics. Finally, the β -cyclodextrin and venetoclax inclusive complex was subject to molecular dynamics simulation for 100 ns to find the RMSD and RMSF of both beta-cyclodextrin and venetoclax. Briefly, the Desmond module, Schrodinger 2022-4 was used to perform molecular dynamics simulation, where the β -CDs and venetoclax inclusive complex were placed inside an orthorhombic box, with a 10 Å thick solvent layer using an explicit water model TIP4P. After conducting molecular dynamics for a duration of 100 ns, the system was kept at a temperature of 300 K. To maintain a pressure of 1.013 bar, the Nose-Hoover Chain thermostat and Martyna-Tobias-Klein barostat were utilized. After the simulations, the trajectory was generated, which was used to calculate the RMSD plots, and RMSF on atom index to indicate the stability of the β -CD-Venetoclax inclusive complex.

2.3. Analytical method development

The UV detector was equilibrated at 25 °C, and a 10 μ L aliquot of the sample was introduced into the HPLC system for the purpose of analyzing the chromatographic peak. Calibration curves were systematically generated by plotting observed peak areas against varying concentration of venetoclax (VEN), and subsequent linear regression computations were conducted. The resulting linear equation, derived from the calibration curves, was subsequently applied to determine the concentration of unknown test samples. This methodological approach ensures precision and accuracy in the quantification of venetoclax, and the presentation adheres to professional scientific writing standards while maintaining unique content.

The development of the analytical methodology for venetoclax involved the utilization of the High-Performance Liquid Chromatography (HPLC) technique (Shimadzu Corporation, Kyoto, Japan). The C18 reverse phase column with dimension of 4.6 \times 150 mm and 5 μ m packing size was selected and maintained at a constant temperature of 25 °C throughout the method development process. The mobile phase contains mixture of acetonitrile (ACN) and 10 mM ammonium acetate aqueous solution (pH 7.5), with 90:10 (v/v) ratios were used. The column underwent conditioning with the mobile phase for 1 h at 1 mL/min flow rate by maintaining room temperature (RT). The UV's detector was equilibrated at 25 °C and 10 μ L of sample was injected in HPLC for analyzing the chromatographic peak. The calibration curves were systematically generated by plotting the observed peak area against varying concentration of VEN and subsequent linear regression computations were conducted. The linear equation was later used to calculate the concentration of the unknown test samples. The analytical assessment of venetoclax (VEN) was conducted employing a UV-visible spectrophotometer (JASCO V-650, India). Equipped with 1 cm quartz cells, the instrument facilitated the determination of absorbance across varying concentration of the samples. A calibration curve, establishing a relationship between concentration and absorbance, was meticulously constructed. It is a quick, economic and useful way to analyze the samples and take accurate measurement of small concentration of samples due to the presence of high sensitivity of photomultiplier tube detector (Sambasevam et al., 2013).

2.4. Preparation of venetoclax and HP- β -CDs cyclodextrin complexes

The generation of inclusion complexes involving venetoclax (VEN) and hydroxypropyl- β -cyclodextrins (HP- β -CDs) was executed utilizing the kneading method. The procedure involved the weighing of drug and HP- β -CDs at various ratios, namely 1:1, 1:2, 1:3, and 1:4. Initially, HP- β -CDs were introduced into a mortar, followed by the addition of a water: acetonitrile (ACN) mixture in a volumetric ratio of 50:50. The resulting slurry underwent kneading for approximately 10 min. At pre-determined intervals, incremental quantities of VEN in powdered form were introduced into the mixture, while concurrently incorporating the solvent-water blend. Subsequent to each addition, the slurry underwent a further kneading (trituration) process lasting approximately 45 min. Ultimately, the resulting semi-solution form was subjected to drying in a vacuum dryer at approximately 40 °C \pm 10 °C for a duration of 48 hrs. This methodology, as detailed by Chaudhary & Pharmacy in 2013 and Garnero et al. in 2014, represents a systematic approach to the development of inclusion complexes, ensuring the formation of stable and controlled structures with varying drug-to-HP- β -CD ratios (Chaudhary & Pharmacy, 2013; Garnero et al., 2014).

2.5 Characterization studies

An extensive analysis of the plain drug, excipients, and cyclodextrin complexes (VEN- HP- β -CD) was conducted utilizing a

diverse array of analytical techniques. These included optical microscopy, Scanning Electron Microscopy (SEM), Fourier Transforms Infra-Red Spectroscopy's (FTIR), Nuclear Magnetic Resonances (NMR) and Differentials Scanning Calorimetry's (DSC), among others. This multifaceted approach ensured a comprehensive characterization of the physical, morphological, and spectroscopic attributes of the plain drug, excipients, and the prepared cyclodextrin complexes, providing valuable insights into their structural and compositional features.

2.5.1. Optical microscopy

Microscopic observation of VEN, HP- β -CDs, physical mixture and drug loaded cyclodextrin complex were performed under a microscope (Nikon Eclipse, China). Initially, the samples were affixed to a microscopic glass slide and observed under a magnification of 45 \times , with accompanying images captured using a digital camera. Subsequently, minute fragments of each particle were compressed between two microscopic slides (Nikon Eclipse, China), and positioned on the stage for further observation. High-resolution photographs were acquired using a Nikon digitalized camera as well as noted by utilizing software's images Nikon NIS-Element (Mallardo et al., 2016). This methodical microscopic analysis facilitated a detailed examination of the morphological characteristics of VEN, and HP- β -CD and their respective complexes.

2.5.2. Attenuated Total Reflectance (ATR) – Fourier Transform Infrared Spectroscopy's (ATR-FTIR's)

The determination of chemical functional groups in Venetoclax, HP- β -D, Cyclodextrin inclusion complex, and physical mixtures was accomplished through Attenuated Total Reflectance Fourier-Transform Infrared Spectroscopy (ATR-FTIR). A Perkin Elmer FTIR's spectrophotometers (Perkin-Elmer 783, Pyrogon's 1000 Spectrophotometers, Shelton, Connecticut, USA) was employed for recording the spectra. This analytical approach is pivotal for forecasting potential interactions, specifically the guest-host interaction between the drug (guest molecules) with cyclodextrin (host components) in solids states. The powdered form of plain drug, HP- β -CD's, cyclodextrin complexes, and physical mixtures were directly subjected to ATR-FTIR analysis, with measurements conducted within the range of 400–4000 cm^{-1} . The *sspec* software was adeptly configured to collect and analyse the results, facilitating the recording of absorption band intensity, shape and position of various samples (Chary et al., 2022; Vaidya et al., 2019).

2.5.3. Nuclear magnetic resonance (NMR)

The structure elucidation of plain drug, excipients, physical mixture and cyclodextrin complex was determined using NMR spectroscopy (500 MHz Avance III Bruker NMR spectrometer instrument, USA). Initially, five (5) mg of sample was dissolved in deuterated dimethyl sulfoxide (DMSO) and subjected for analyzing the sample. The resulting NMR were meticulously analyzed using MestReNova software, enabling

the calculation of chemical shifts values, which further defines the functional group's available in the samples (Gao et al., 2019).

2.5.4. Differential scanning calorimetry (DSC)

Thermometric analysis of the samples was conducted using the differential scanning calorimetry (DSC-3 Star, METTLER Toledo, USA). Approximately 4–5 mg of each sample was meticulously placed into an aluminum pan, sealed, and accompanied by a reference. The sample unit cell underwent nitrogen gas purging at a flow rate of 30 mL/min to facilitate rapid cooling. The experimental protocol commenced with an incremental temperature increase from 10 to 300 °C at a heating rate of 10 °C/min. To ensure precision and reliability, the measurements were executed in triplicate series.

2.5.5. Scanning electron microscopy (SEM)

The surface morphology of the drug, excipient, physical mixture, and cyclodextrin inclusive complex was analyzed using Scanning Electron Microscopy's (FEI Quanta 250, Netherlands). The procedure involved placing the samples on double-sided adhesive carbon tapes, followed by a coating with gold through three cycles to enhance the conductivity using an ion sputter chamber. Subsequently, the samples underwent bombarded with electronic beams at 10 Kev (excitations energy's) and the images were recorded at specific magnifications (Garnero et al., 2012).

2.5.6. Powder X-ray's diffraction (PXRD's)

PXRD patterns of various samples were determined by utilizing diffractometer (Malvern Panalytical's X-ray diffractometers, U.K. Almelo, Netherlands) measured at 25° C. Cu K α sources produce a geometric beam that runs parallel across primary and secondary solar slits. X-ray's scattering beams were functioned at 40 KV and 25 mA. A specific amount of sample was positioned on to 25-mm poly-methyl methacrylate holders and spreads a steady state layer over the holder. Angular ranges spanning from 5° to 60° 2 θ were employed to determine the X-ray scattering pattern with scanning rates set at 0.2 °C/min. The resulting diffractogram of the respective sample were analyzed by utilizing OriginPro (version 8.5 and produced by OriginLab Corporation, runs on Microsoft Windows) software. This software used for interactive scientific graphing and data analysis in XRD (Abarca et al., 2016; Hidau et al., 2017).

2.6. Entrapment efficiency and drug loading capacity

The entrapment efficiency (EE) and drugs loading capacity (DLC) was performed by measuring the amount of VEN that entrapped into the cyclodextrin complex. The fixed amount of formulation was dissolved in 1 mL of solvent and incubated for 24 hrs. After completion of incubation period, the samples were centrifuged (Eppendorf, Hamburg, Germany) at 3500 rpm for 30 min, followed by collection of supernatant liquid from the respective samples and subjected for

quantification using analytical HPLC method (Salih et al., 2019; Torres-alvarez et al., 2020). However, the %EE and %DLC were calculated by using the following equation and reported as mean and SD value and run-in triplicate series ($n=3$).

$$\text{EE\%} = \frac{\text{Total drug weight} - \text{Free drug weight}}{\text{Total drug weight}} * 100$$

$$\text{DLC\%} = \frac{\text{Entrapped drug weight}}{\text{Loaded drug weight} + \text{weight of feeding polymer}} * 100$$

2.7. In-vitro drug release studies

Dialysis membrane method was employed to perform *in-vitro* drugs release studies of pure VEN suspension and VEN-HP- β -CD complex. The release media was composed of phosphate buffer solution (6.8 pH) added with 0.5% non-ionic surfactant i.e., Tween[®] 80. The inclusion complex and free drug suspension (equivalent to 1 mg/ml) was loaded into dialysis bag and hermetically tied with the help of dialysis clips and placed into 50 mL Schott Duran bottle consisting of release media subjected for orbital shaking incubator (IKA, Germany) with 100 rpm maintained at $37 \pm 0.5^\circ\text{C}$. At specified times interval (0.083, 0.166, 0.25, 0.5, 0.75, 1, 2, 4, 6, 8, 12 and 24 hrs) aliquot samples (1 mL) were collected and replaced with pre-incubated freshly prepared buffer media (1 ml) at constant temperature. Simultaneously, these collected samples were quantified by using HPLC (Al-abboodi et al., 2021). The different types of drug kinetic models such as Zero order, first order, Hixon Crowell model, korsmeyer-peppas model, Higuchi model were performed for explaining the drug release mechanism of Venetoclax from cyclodextrin complex.

2.8. In-vitro cytotoxicity study

2.8.1. Cell culture

A-549 (human's lung epithelial cancer cells) had been procured from National Centre for Cell Science (NCCS), Pune, India. This cells line was grown in appropriate media of 90% RPMI, 10% Fetal bovine serum (FBS), 1% Penicillin streptomycin antibiotic solution, 1% trypsin solution. The A-549 cells were maintained at 98% relative humidity (RH) as well as 5% CO₂ at 37 °C in an incubator (IKA, Germany).

2.8.2. MTT (3-(4, 5-dimethylthiazol-2-yl)-2, 5-diphenyltetrazolium bromide) assay

The *in-vitro* cell cytotoxicity assay was performed for both Venetoclax suspension and VEN-CDs inclusion complex (1:2 ratio) using A-549 lung epithelial cell lines. Initially, A-549 cells were cultured in 96 well plates using RPMI media, supplemented with 10% Fetal bovine serum (FBS) and 1% Penicillin streptomycin antibiotic solution, 1% trypsin solution with a density of 4×10^3 cells/well and incubated for overnight using incubator maintained at 37 °C, supplied with CO₂ gas. After incubation period the media from the culture plate was removed and these cells were treated with VEN,

and formulation (VEN-HP- β -CD) at various concentrations using pre-warmed fresh media without any FBS content in it and subjected for incubation for a period of 24 hrs and 48 hrs. After completion of incubation period, the media was removed and 20 μl of 3-(4,5-Dimethylthiazol-2-yl)-2,5-Diphenyltetrazolium Bromide (0.5 mg/ml) was added and incubated for 4 hrs, by maintaining at 5% CO₂ and 37 °C. After incubation period, MTT reagent was withdrawn from each well and added with 100 μl of DMSO to each well for dissolving formazan crystals. Finally, these 96-well plate was subjected for Multimode Plate Reader (Perkin Elmer, EnVision) for measuring absorbance of each well at 570 nm wavelength, and IC₅₀ values were derived by plotting concentration against %inhibition (Lodgekar et al., 2019).

2.8.3. Qualitative cell apoptosis assay

2.8.3.1. DAPI staining studies. The cell apoptosis assay was performed using DAPI staining in which the 12-well plates were taken, and 1×10^5 cells per well of A-549 cells were seeded and incubated overnight. The immediate day, the cells were treated with IC50 dose and high dose of venetoclax loaded cyclodextrin. Following a 24-hrs incubation period, the cells underwent three washes with a pH 7.4 PBS solution. Subsequently, a 4% paraformaldehyde solution was used to treat the cells for 30 min. The cells were then stained with a DAPI solution and examined under a fluorescent microscope at 20 \times magnification, using a blue filter. This process ensured that the cells were adequately prepared for further analysis (Chary et al., 2022).

2.8.3.2. Reactive Oxygen Species (ROS) assay. The green fluorescent dye DCFDA (2',7'-dichlorofluorescein diacetate) is utilized to detect the presence of Reactive Oxygen Species (ROS) within cells. DCFDA, initially non-fluorescent, undergoes deacetylation by esterases upon entry into cells, and subsequently reacts with ROS, resulting in the production of green fluorescence. Briefly, the A-549 cells were seeded at a density of 1×10^5 cells per well in a six-well plate and allowed to adhere overnight. The immediate day, the cells were treated with an IC50 dose and a high dose of venetoclax loaded cyclodextrin. The cells were subjected to three washes with a pH 7.4 PBS solution, following a 24-hrs incubation period. Next, the cells were treated with 10 $\mu\text{g/ml}$ of DCFDA and incubated for 30 min. After the incubation period, the cells were examined using a fluorescent microscope with a green filter, at a magnification of 20 \times (Chary et al., 2022).

2.8.3.3. Immunofluorescence assay. To begin, A-549 cells were seeded into cell imaging chambers and incubated for a 24-hrs period. The cells were then treated with a drug-loaded formulation at an IC₅₀ dose. To prepare the cells for further analysis, they were fixed with 4% paraformaldehyde, permeabilized using Triton-X-100, and blocked using 3% bovine serum albumin (BSA). Next, a primary antibody for caspase-9 was added to the cells and allowed to incubate overnight. A FITC-conjugated secondary antibody was used

to detect the primary antibody. Finally, the prepared slides were mounted using Fluoroshield™ with DAPI histology mounting medium (Sigma-Aldrich), and images were captured at a magnification of 10X using a fluorescence microscope. This rigorous preparation ensured that the cells were optimally primed for further analysis (Chary et al., 2022).

2.9. In-vivo pharmacokinetic studies

The protocol required for the initiation of animal studies was approved by the Institutional Animal Ethics Committee and NIPER Hyderabad, India. The CPCSEA guidelines were strictly followed while conducting the experiments on the procured animals. The in-vivo pharmacokinetic studies were performed in Wistar rats weighing 200–250 g. All rats were caged and permitted to acclimatize at room temperature ($25 \pm 1^\circ\text{C}$), $55 \pm 5\%$ relative humidity, and 12 h light/dark cycle before commencing the study. All rats were provided with water and food *ad libitum*. The animals were randomly divided into two groups; the first group ($n=6$) orally received VEN-HP- β -CD complex at a dose of 25 mg/kg, whereas the second group ($n=6$) orally received VEN suspension (0.5% tween 80) at a dose of 25 mg/kg. At pre-determined time points (0, 0.25, 0.5, 1, 2, 4, 6, 8, 12, 24 and 48 hrs), the blood samples (200 μL) were collected by retro-orbital puncture into the centrifuge tubes having sodium citrate (3.8% w/v) as an anti-coagulant. The samples were centrifuged at $10,000 \pm 50$ rpm for 10 min to separate plasma, followed by storage at -20°C until HPLC analysis. The VEN concentrations in rat plasma were analyzed as a function of time by PK Solver 2.0 Add-in, Excel 2019. The non-compartmental analysis (NCA) model was used to compute the pharmacokinetic parameters.

2.10. Statistical analysis

The experiments were performed in triplicate ($n=3$) to achieve accurate and reliable results. The mean and standard deviation were calculated from the experimental values obtained. GraphPad InStat Software (Version 6.00, GraphPad Software, San Diego, California, USA) was employed to analyze the data, using one-way ANOVA to determine statistical significance with a p value of ≤ 0.05 . This statistical analysis ensured that the results were statistically significant and robust.

3. Results and discussion

Cyclodextrin comprises non-reducing oligosaccharides with a cyclic structure made up of glucopyranose units. It has derivatives like α -, β -, and γ -cyclodextrins, which showed greater actions as compared with the larger molecules of cyclodextrins. They are widely used in pharmaceutical industry, and it has a significant application for enhancing the solubility as well as bioavailability of poorly aqueous soluble drugs by complex formation (Haimhoffer et al., 2019). Cyclodextrin acts as desirable formulations to improve the stability and solubility of food additives and natural ingredients. Molecular encapsulation of hydrophobic drugs in the cyclodextrin cavity (CDs) provides stabilizing environment (Fang et al., 2020).

We have successfully developed the stable cyclodextrin inclusion complex of venetoclax and exhaustively characterized. The cyclodextrin inclusion complex shows high drug loading capacity and sustained drug release, which is an important and prerequisites for cancer therapy.

3.1. Phase solubility

Phase solubility study was carried out to forecast stability constants and stoichiometric ratios of inclusion complex (VEN-HP- β -CD) formulation. The solubility of plain VEN suspension was 0.000933 mg/mL (practically insoluble and fall in BCS class-IV). The results depicted in Figure S1 indicate the formation of a cyclodextrin complex of HP- β -CD with VEN at 0.001 mM concentration. Upon observing the phase solubility curve, the solubility of VEN in HP- β -CDs was drastically increased to 0.01 mM and decline with respective to excipient concentration. According to Higuchi and Connor's classification curve was categorized under the AL type (enhanced in solubility of drug for a purpose of cyclodextrin concentration). The solubility of VEN in HP- β -CDs was increased to 3.16 folds as compared to pure VEN, as illustrated in Figure S1.

3.2. Molecular modelling data

Herein, we carried out molecular docking studies to predict the inclination of the firm chemical structure of the venetoclax-HP- β -CD's inclusion complexes. The docking study had displayed that 4-methylpiperazine group of venetoclax is oriented into the cavity of HP- β -CD's, docking poses of the venetoclax revealed as combination of hydrophobic as well as electrostatic non-bonded interaction maintain the venetoclax-HP- β -CD complexes, as shown in Figure 1. While pyrrolo-[2.3-b] pyridine and 3-nitro-4-((tetrahydro-2H-pyran-4-yl) methyl) amino benzene sulfonamide segments of Venetoclax remained outside the HP- β -CD's cavity. The molecular docking was performed to understand the possible interaction between HP- β -CD and venetoclax inclusion complex. During molecular docking, the best docking poses refer to the XP glide score and docking score. After Venetoclax preparation, two possible ionization states (Figure 1A) were generated were subjected to the Extra Precision (XP) docking with minimized HP- β -CD to get best docking score and glide score. First ionization state of venetoclax was observed to have best docking and making best interactions include Hydrogen bonds and Aromatic Hydrogen bonds (Figure 1C) as compared to second ionization state. MM-GBSA was used to find venetoclax affinity toward HP- β -CD, results were in Table 1. After this, the best docking state of HP- β -CD and Venetoclax inclusion complex was subjected to Molecular dynamics stimulations for 100 ns to denotes complex stability. We observed HP- β -CD and Venetoclax inclusion complex was stable by plotting RMSD and RMSF values of HP- β -CD and Venetoclax and also observed possible interactions (Hydrogen bonds and Halogen bonds) (Figure 1B) based on the trajectory generated after Molecular stimulations, docking score and binding energies of the prepared cyclodextrin complex as shown in Table 1.

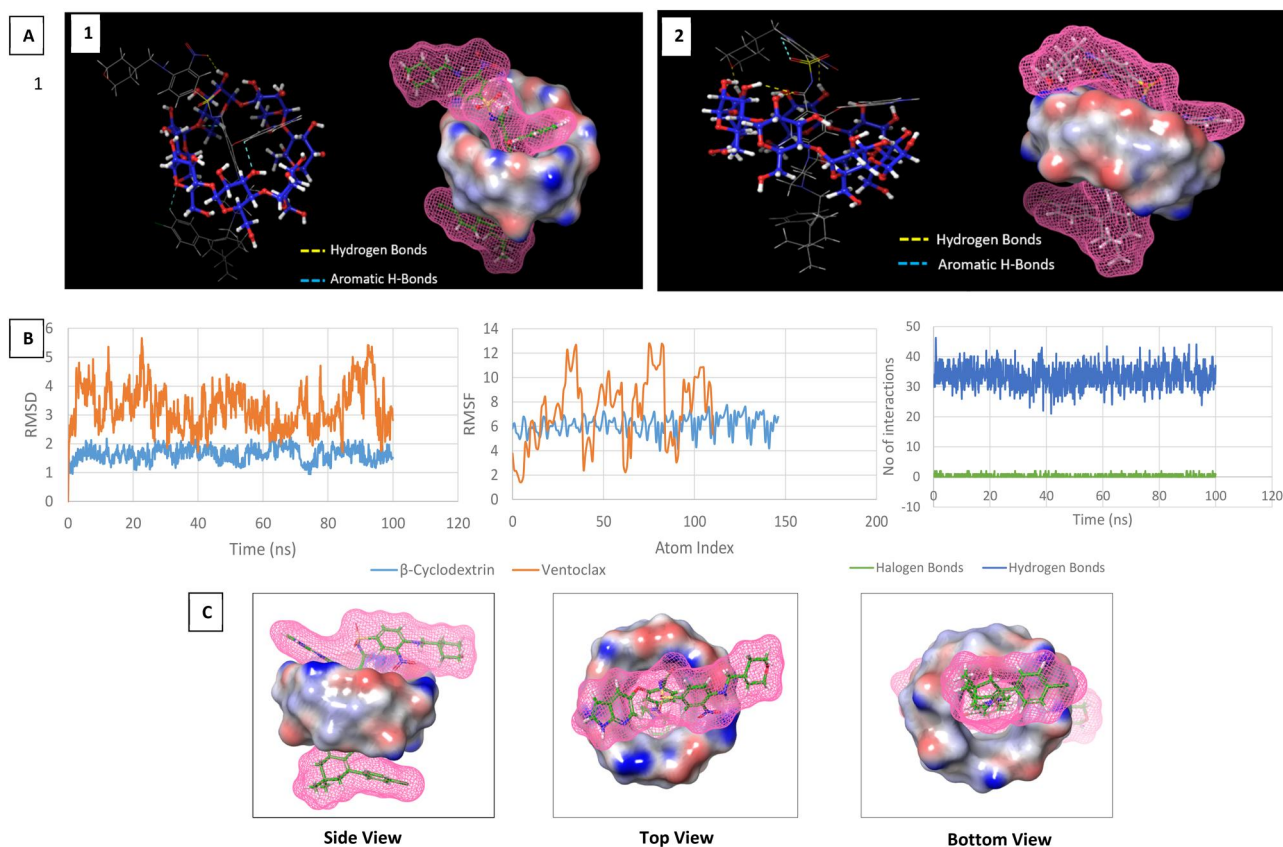


Figure 1. (A) Venetoclax ionization states showing two different forms, (B) RMSD plot of β -Cyclodextrin and Venetoclax inclusion complex during the molecular dynamics for 100 ns and RMSF value based on Atom index during trajectory frames, (C) Representation of β -Cyclodextrin and Venetoclax inclusive complex in different views.

Table 1. MM-GBSA binding energies and docking results.

Venetoclax ionization states	Docking score (kcal/mol)	XP GScore (kcal/mol)	glide gscore (kcal/mol)	ΔG Bind (kcal/mol)	ΔG Bind Colomb (kcal/mol)	ΔG Bind H Bond (kcal/mol)	ΔG Bind Lipo (kcal/mol)	ΔG Bind vdW (kcal/mol)
1	1.346	-1.48	-1.48	-58.07	-2.18	-1.03	-25.31	-51.95
2	3.136	3.30	3.30	-53.53	0.24	-0.88	-29.20	-47.02

3.3. Analytical method development

A successful development and optimization of an analytical method for VEN were achieved by considering various process parameters such as retention time, tailing factor, symmetry of peak. The parameters were optimized on the basis of sharpness of drug peak, tailing factor, retention time and constant area of chromatographic peak having same concentration. The mobile phase employed was a mixture of acetonitrile and 10 mM ammonium acetate aqueous solutions, 90:10 (v/v) ratios. The mobile phases were raised at 1 mL/min and R_t was found to be 6.3 min observed at λ_{max} 275 nm and linear regression was given as $y = 24346x + 4934.7$ with $R^2 = 0.9993$ as shown in Figure S2. UV spectrophotometer is the simple technique for the measurement of absorbance, transmittance and wavelength of a chromophore containing substance. The UV spectra of VEN were recorded at wavelength of 275 nm. The linearity and regression values were observed at $y = 0.0473x - 0.0255$ and 0.9922. The enhancement in absorption intensity, characterized by the occurrence of hyperchromic peak in cyclodextrin complexes without any changes in λ_{max} , indicated the formation of the complex.

The complete spectral analysis was carried out at fixed wavelength and UV calibration graph shown in Figure S3.

3.4. Preparations of VEN and HP- β -CD's inclusion complexes

A comprehensive investigation was conducted to identify an optimal method for preparing the cyclodextrin inclusion complex. The complexation between drug and excipient were formulated by various methodologies like solvents evaporation technique, freeze drying and kneading method as well. From these, solvent evaporation (rotary evaporation) method resulted the decrease in product yield, freeze drying method was not suitable for water insoluble drugs for formulating cyclodextrin complex. Laterally, complexes were prepared with uniform mixing i.e., kneading method, in which % yield of complex product was more i.e., 50%, due to proper uniform mixing of drug and excipient, forms tight boundation of complexation in between. These methods were tried to formulate cyclodextrin inclusion complex using various stoichiometric ratios such as 1:1, 1:2, 1:3 and so on.

Out these ratios cyclodextrin complex (1:2 stoichiometric ratio) showed complex formation by using kneading method. The diagrammatic representation of cyclodextrin complexes were showed in Figure 2.

3.5. Characterization of venetoclax loaded cyclodextrin by optical microscopy, ATIR-FTIR, NMR, DSC, SEM & XRD

Optical microscopy was performed for VEN, HP- β -CDs, physical mixture and VEN-HP- β -CDs cyclodextrin complex to observe the morphological behavior. From Figure 3, VEN exhibited an irregular rigid form; HP- β -CDs resembles spherical shape, whereas the complexes of VEN-HP- β -CDs formulated by kneading method appeared to be cylindrical shaped crystals. In the physical mixture, both the drug and excipient seemed to exist as distinct entities. From this morphological behavior, it was assessed that drug (VEN) and excipient particles underwent a change in their morphological shapes upon the formation of the cyclodextrin complex.

The use of ATR-FTIR technique facilitated the identification of solid inclusion complex formation and their functional groups within the inclusion complex, by analyzing the positions and shapes of absorbance bands in VEN, HP- β -CDs, physical mixtures, cyclodextrin complexes of VEN-HP- β -CDs. Critical attributable peaks for Venetoclax were recorded at 3700–3400 cm^{-1} region, N–H stretched vibration (3364 and 3303 cm^{-1}), C–H stretched vibrations of the benzene rings (3141 and 3105 cm^{-1}), C–H stretched vibrations of CH_2 and CH_3 groups (2917 and 2842 cm^{-1}), C=O stretching vibration of an amide bond (1677 cm^{-1}), and stretching vibrations that are probably associated with C=C aromatic rings, the $-\text{NO}_2$ group, and the $-\text{SO}_2$ group (1607, 1569, 1521, 1362, 1346 and 1141 cm^{-1}) these characteristic peaks confirm to be VEN and HP- β -CD characteristic peaks were found to be 2926, 1738, 1606, 1364, 1217, 1085, 1027, 836

and 563 cm^{-1} . The VEN-HP- β -CD's inclusion complexes showed IR peaks in ranges of 3339.77 cm^{-1} to 576.39 cm^{-1} and characteristic peak of NO_2 group showed at 1607 cm^{-1} with a less intensity than that of pure drug, this complex showed major characteristic peaks with stretching and bending at different groups. Hence, it conforms the enmasking of VEN in HP- β -CD complex, as shown in Figure 4.

NMR is used to analyze the samples according to their chemical shifts values and displayed interactions formed between two peaks. The VEN, HP- β -CD's, physical mixture of VEN-HP- β -CDs and cyclodextrin complex of VEN-HP- β -CDs has been analyzed by proton NMR. The chemical shift values of VEN recorded as δ 11.70 (s, 14H), 8.60 (dd, $J=17.3$, 11.4 Hz, 21H), 8.57 (d, $J=1.6$ Hz, 11H), 8.56 (s, 6H), 8.05 (d, $J=2.6$ Hz, 17H), 7.82 (s, 5H), 7.82 (s, 2H), 7.80 (s, 3H), 7.80 (s, 3H), 7.54 (d, $J=2.4$ Hz, 12H), 7.52 (dd, $J=10.0$, 7.0 Hz, 26H), 7.52–7.48 (m, 23H), 7.36 (d, $J=1.8$ Hz, 14H), 7.34 (s, 17H), 7.13 (s, 5H), 7.13 (s, 5H), 7.12 (d, $J=9.4$ Hz, 14H), 7.12 (d, $J=9.4$ Hz, 10H), 7.05 (s, 13H), 7.05–7.03 (m, 16H), 6.70 (s, 4H), 6.68 (d, $J=2.2$ Hz, 8H), 6.40 (dd, $J=3.3$, 1.8 Hz, 15H), 6.20 (d, $J=2.1$ Hz, 14H), 3.87 (d, $J=2.4$ Hz, 10H), 3.87–3.83 (m, 23H), 3.33 (s, 165H), 3.31 (s, 31H), 3.27 (d, $J=1.5$ Hz, 17H), 3.26 (d, $J=10.1$ Hz, 18H), 3.08 (s, 56H), 2.76 (s, 30H), 2.55 (s, 3H), 2.51 (dt, $J=3.6$, 1.8 Hz, 122H), 2.21 (s, 49H), 2.15 (s, 41H), 1.94 (d, $J=13.8$ Hz, 31H), 1.63 (s, 13H), 1.62 (d, $J=12.7$ Hz, 26H), 1.39 (t, $J=6.4$ Hz, 33H), 1.32–1.28 (m, 7H), 1.28–1.21 (m, 27H), 0.93 (s, 86H), 0.86 (d, $J=6.6$ Hz, 3H). The chemical shift values of HP- β -CD with their number of protons were found to be δ 5.11–4.97 (m, 20H), 4.84 (s, 19H), 3.75 (s, 42H), 3.62 (s, 131H), 3.35 (s, 108H), 3.33 (s, 7H), 2.52 (s, 4H), 2.51 (s, 8H), 2.51 (s, 17H), 2.51 (s, 12H), 2.50 (s, 6H), 1.01 (d, $J=17.5$ Hz, 74H).

The chemical shift values of physical mixture were found to be δ 8.61 (s, 4H), 8.56 (d, $J=2.0$ Hz, 4H), 8.04 (d, $J=2.5$ Hz, 4H), 7.81 (s, 2H), 7.80 (d, $J=7.8$ Hz, 4H), 7.52 (s, 1H), 7.51 (s, 2H), 7.49 (s, 1H), 6.39 (dd, $J=3.2$, 1.8 Hz, 4H), 6.20 (d, $J=1.9$ Hz, 4H), 5.04 (s, 15H), 4.85 (s, 18H), 4.54 (s, 33H), 4.46–

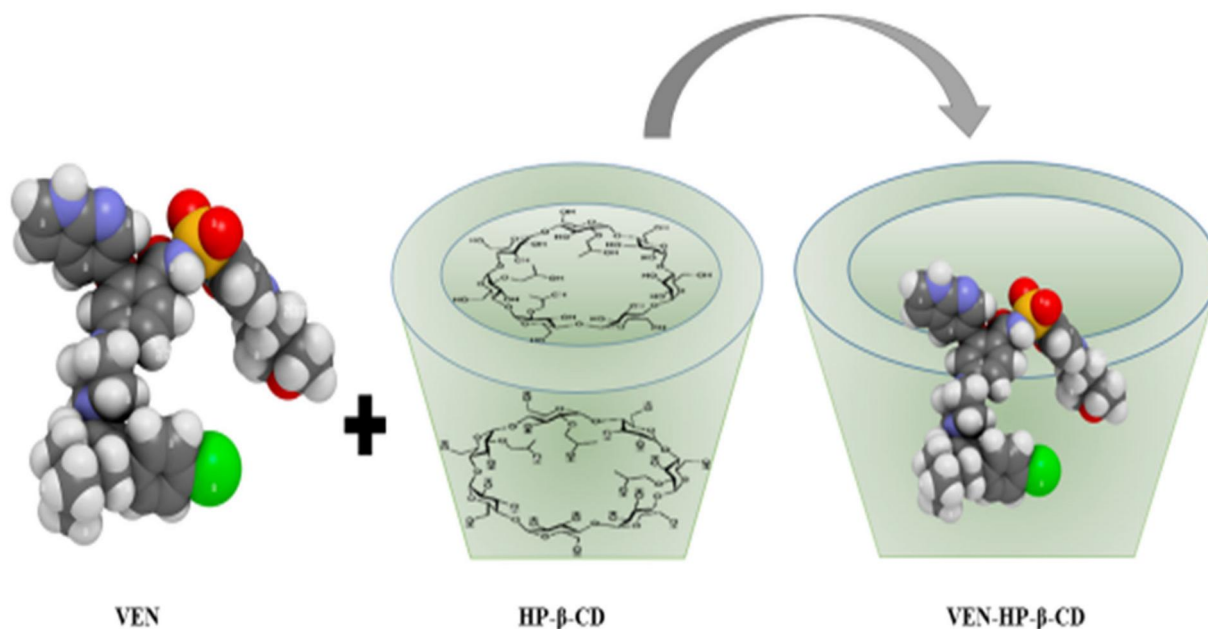


Figure 2. Preparations of VEN-HP- β -CD inclusion complex.

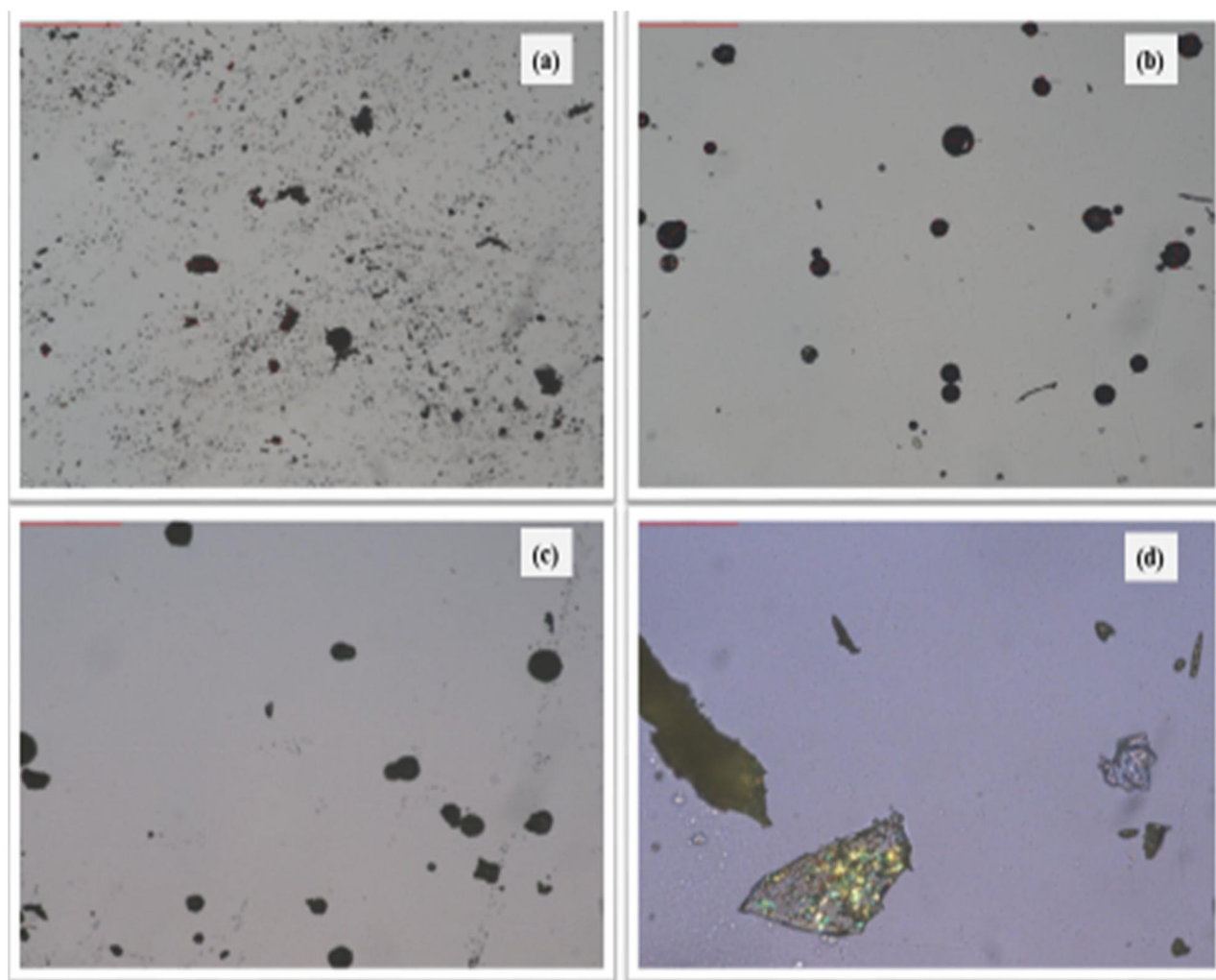


Figure 3. Images obtained from optical microscopy at magnification of 45X showing (a) Venetoclax (VEN), (b) HP- β -CD, (c) VEN-HP- β -CD physical mixture, (d) VEN-HP- β -CD cyclodextrin complex.

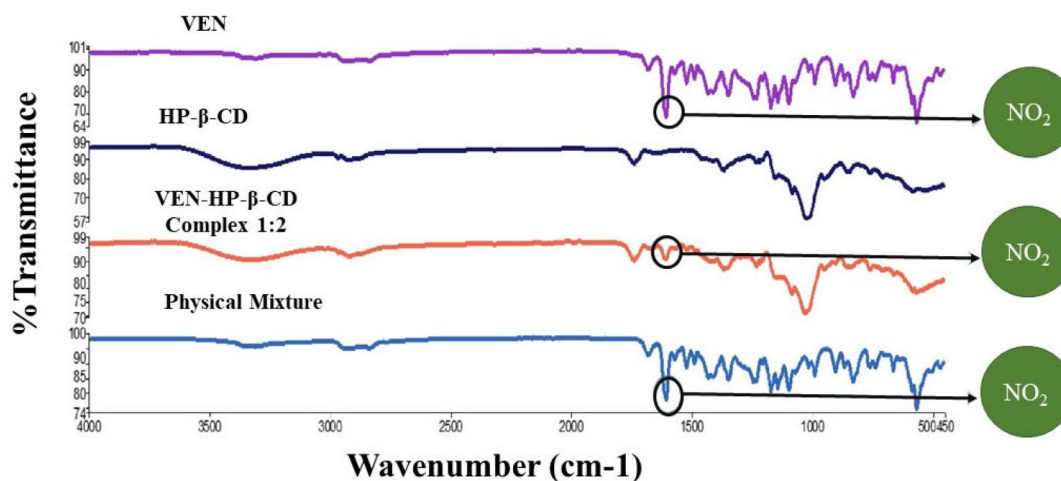


Figure 4. Overlay of FT-IR spectrum shows characteristic peaks of VEN, HP- β -CDs, VEN- HP- β -CDs physical mixtures and VEN-HP- β -CDs inclusion complexes.

4.41 (m, 4H), 3.96–3.79 (m, 27H), 3.86–3.81 (m, 14H), 3.62 (s, 73H), 3.60–3.50 (m, 58H), 3.34 (s, 115H), 3.32 (s, 9H), 3.31 (s, 8H), 3.30 (s, 8H), 3.27 (s, 5H), 3.08 (s, 17H), 2.95–2.91 (m, 1H), 2.75 (s, 9H), 2.51 (s, 12H), 2.51 (s, 15H), 2.52–2.35 (m, 47H), 2.51 (s, 8H), 2.50–2.50 (m, 5H), 2.15 (s, 8H), 1.96 (s, 7H), 1.61 (s, 5H), 1.63–1.29 (m, 18H), 1.39 (s, 2H), 1.31–1.26 (m, 5H),

1.24 (t, $J=8.0$ Hz, 8H), 1.03 (s, 68H), 0.93 (s, 20H). From these values of physical mixture it was considered that there is no much difference between pure drug. Whereas, VEN- HP- β -CD's inclusions complex it was observed to be δ 8.04 (d, $J=2.5$ Hz, 8H), 7.53 (d, $J=9.4$ Hz, 7H), 7.50 (t, $J=4.7$ Hz, 8H), 7.36 (s, 4H), 7.34 (s, 5H), 6.20 (d, $J=1.9$ Hz, 7H), 3.89–3.85

(m, 10H), 3.84 (d, $J=3.5$ Hz, 9H), 3.32 (d, $J=11.8$ Hz, 424H), 3.08 (s, 34H), 2.51 (dd, $J=3.5, 1.7$ Hz, 191H), 2.20 (s, 21H), 1.96 (s, 16H), 1.72–1.66 (m, 4H), 1.62 (d, $J=8.8$ Hz, 8H), 1.39 (t, $J=6.5$ Hz, 15H), 1.26 (d, $J=14.3$ Hz, 24H), 0.93 (s, 36H). From this complete analysis of chemical shift values, down-field shift was observed in between VEN-HP- β CD cyclodextrin complex (Figure 5). The chemicals shifts of VEN in complexes were well as understandable especially, in cases of H3, H3, H3 and H12 protons of VEN, as shown in Table S1. Up-field shift in chemical shift values of complete protons in VEN rather than H6, whereas down-field shift were noticed in existence of HP- β CDs.

VEN exhibited sharp glass transition peak at 171.1°C indicating its amorphous nature. Physical mixture at 171.1°C revealed a small glass transition peak was observed, which indicated the amorphous behavior of mixture. However, the cyclodextrin complex of 1:2 ratios displayed that there was no peak observed, due to the complete inclusion of VEN into the HP- β -CD. This absence of a peak is indicative of the

formation of guest-host molecule cavity, confirming the successful formation of the VEN- HP- β -CD inclusion complex, as illustrated in Figure 6.

The Scanning Electron Microscopy (SEM) were executed to analyze the shape and surfaces morphology of VEN, HP- β -CDs, physical mixtures of VEN-HP- β -CDs and inclusions complexes of VEN-HP- β -CDs, as shown in Figure 7. However, the shape of VEN analyzed to be irregular with rough surface, HP- β -CDs having circular shape resembles like beads structure possesses particle size in the limit of 10–50 μm , physical mixtures was found to be circular rough shaped particles and the cyclodextrin complexes of VEN- HP- β -CDs revealed as cylindrical shaped with the size range of 40 to 60 μm . However, the irregular shaped drug particle encapsulated into the circular shaped excipient, in turn formed a cylindrical shaped large size particle which may considered as cyclodextrin inclusion complex. It was evident that the small particles of drug incorporated with particles of excipient, which aggregated to

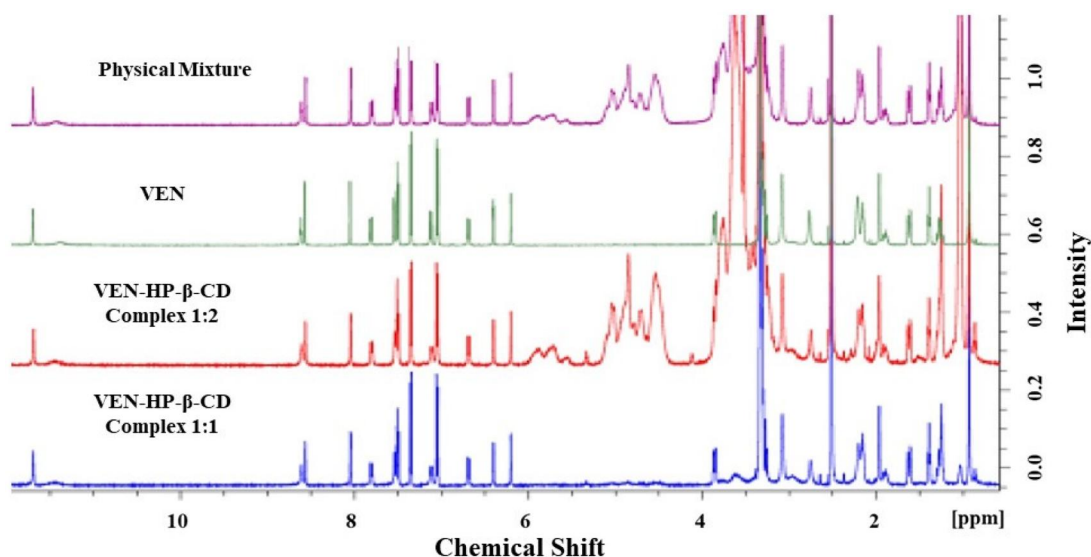


Figure 5. NMR spectrum of VEN- HP- β -CD's physical mixtures, VEN, Inclusion complexes of VEN-HP- β -CD's 1:1 and 1:2.

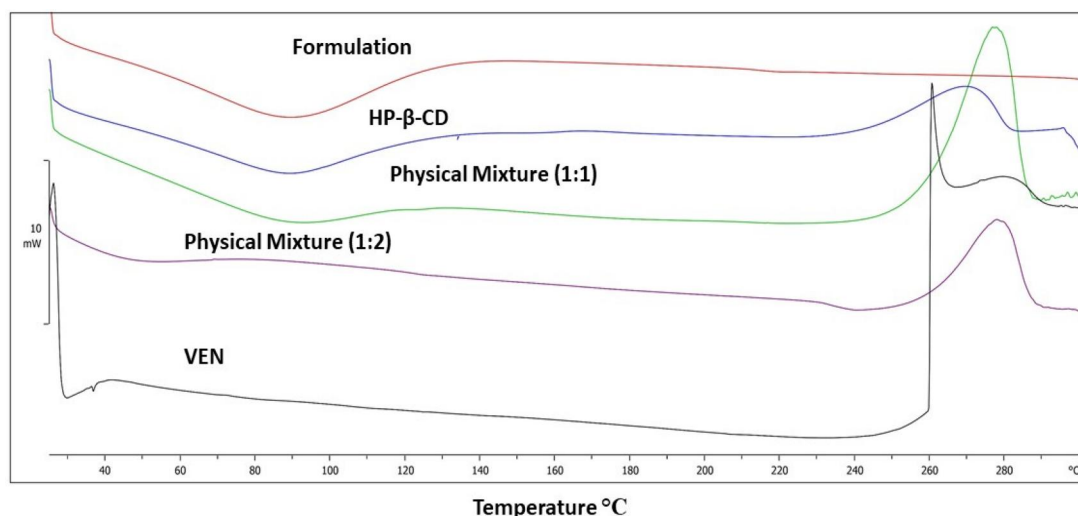


Figure 6. DSC thermogram of VEN, HP- β -CDs, physical mixture of VEN- HP- β -CDs and inclusion complex of VEN- HP- β -CDs.

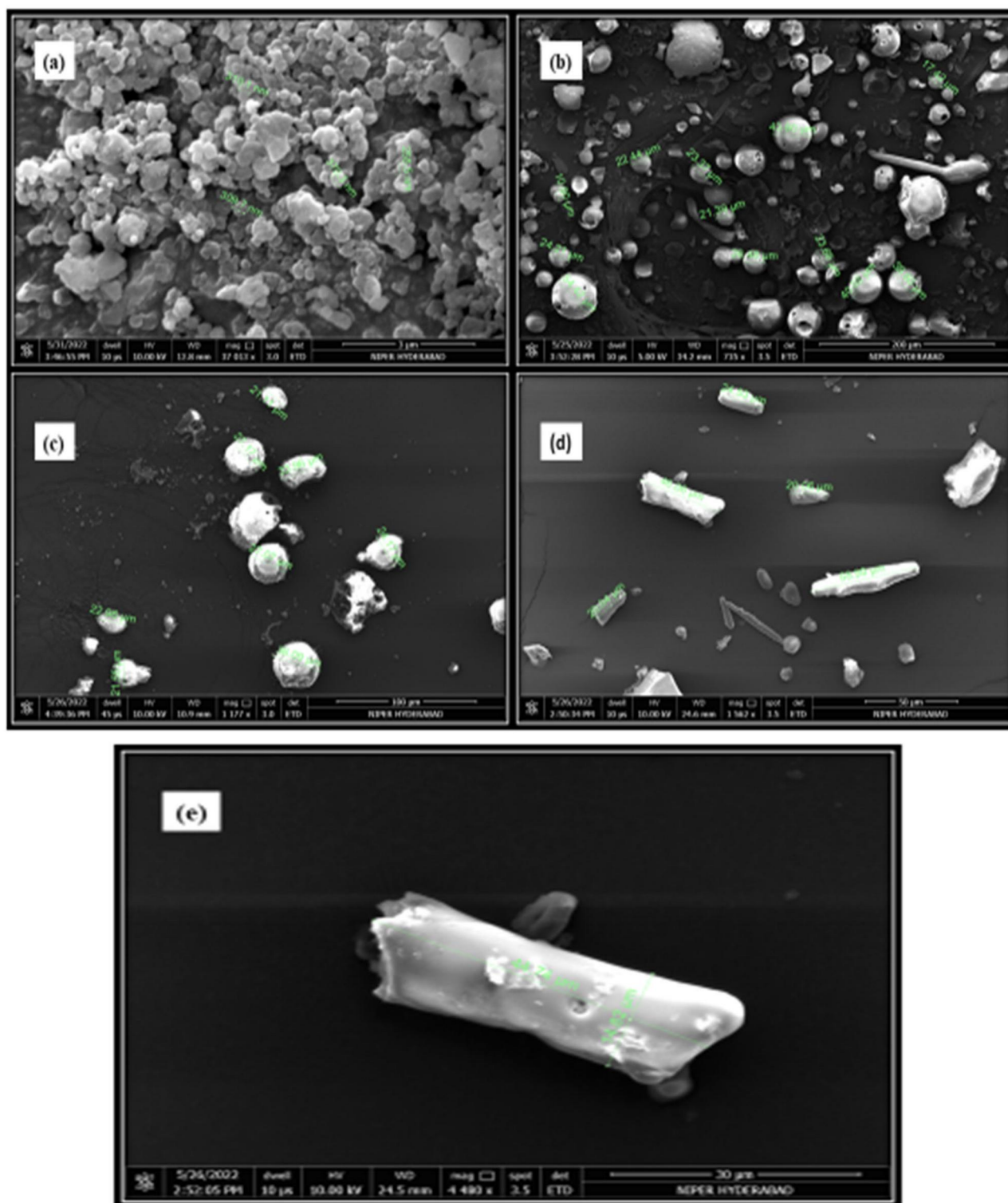


Figure 7. Scanning Electron Micrographs of (a) VEN, (b) HP- β -CDs, (c) Physical mixtures of VEN- HP- β -CDs and (d & e) Inclusion complexes of VEN- HP- β -CDs.

form a large size particle of cylindrical shaped inclusion complex.

Powdered X-rays diffraction (PXRD) helps to confirm the crystalline as well as amorphous behaviour of drugs, excipient and solid inclusion complex. This technique was performed at room temperature. Venetoclax shows halo-form like structure with respect to coupled 2- theta (2θ). Cu Cu Anode was used and the values of k-alpha 1 and k-alpha 2 were analyzed at

1.54060 Å as well as 1.54439 Å and k-beta value of VEN was operated at 1.39222 Å. This halo-form like structure may represented as amorphous nature of drug. The hydroxyl propyl- β cyclodextrin revealed haloform like structure at 2- theta value of 3.002° with same values of k-alpha 1&2 and k-beta values as that of VEN. These halo-form pattern of HP- β -CDs showing its amorphous behaviour. The physical mixtures of VEN- HP- β -CDs revealed halo pattern peaks in it. Furthermore, the

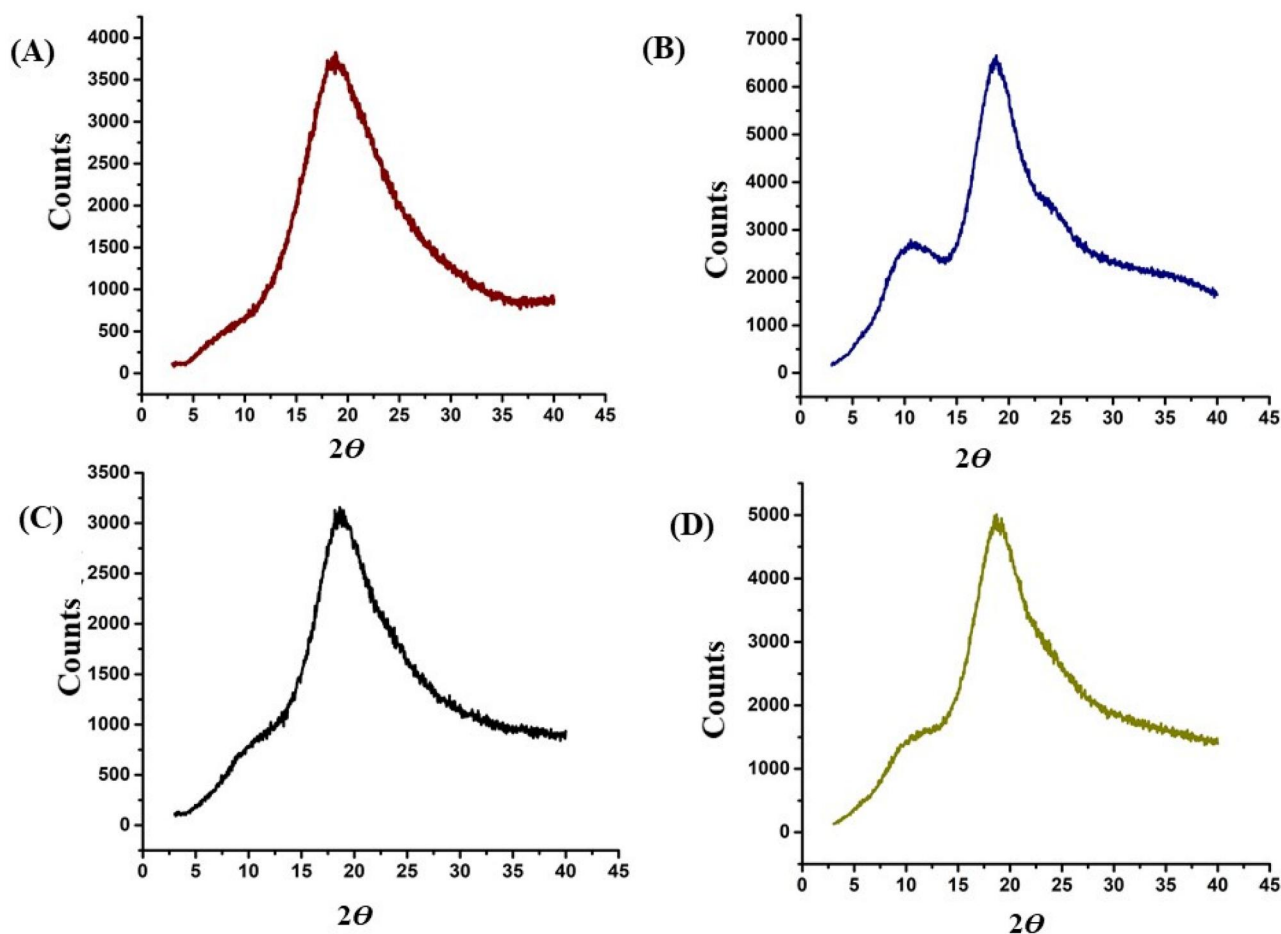


Figure 8. X-ray powder diffraction spectra of (A) VEN, (B) HP- β -CDs, (C) Physical mixture of VEN-HP- β -CDs and (D) cyclodextrin complexes of VEN- HP- β -CDs.

complexation of VEN-HP- β -CDs displayed halo pattern peaks in its solid state. These halo pattern peaks confirm the amorphous nature of cyclodextrin complex as shown in Figure 8. PXRD diffractograms are evident to correlate the DSC thermogram for finding out the molecular dispersion of a component. Where, the DSC thermogram of VEN-HP- β -CDs shows amorphous nature hence, concluding VEN was molecularly dispersed in the cyclodextrin complex.

3.6. Entrapment efficiency and drug loading capacity

The percent entrapment efficacy (EE%) and drug loading capacity (DL%) of VEN in the inclusion complexes of cyclodextrin were calculated using RP-HPLC analytical method. The %EE and %DL of VEN-HP- β -CD inclusion complexes were found to be $95.44 \pm 0.3\%$ and $33.33 \pm 0.2\%$ and it was performed in triplicate series.

3.7. In-vitro drug release data

The drug release studies of the VEN-HP- β -CDs inclusion complex was carried out using dialysis diffusion membrane techniques and showed initial rapid drug release from the inclusion complex formulation as compared with pure VEN suspension. Initially, the formulation of cyclodextrin complex (1:2) was released at faster rate on comparison with pure

VEN. The percentage drug released from formulation was found to be 25% at 60 min, 56% at 12h and 81.65% at 24 hrs, respectively. Whereas 100% drug release was observed at 5 h in case of pure API (VEN) as shown in Figure 9. From these comparison studies, it was confirmed that the release of drug was enhanced on preparation of VEN-HP- β -CD inclusion complex as compared to pure VEN. The release behavior of drug from cyclodextrin complex was successfully determined using numerous kinetics model's such as zero and First order, Higuchi's square root model and Korsmeyer's—Peppas models.

$$\text{Zero order model } Q = K_0 t \dots \quad (\text{i})$$

whereas Q represented the amount of drug release, t notified the time taken by drug to release and K_0 represented as constant for zero order.

$$\text{First orders } \log Q = \log Q_0 - K_1 t / 2.303 \dots \quad (\text{ii})$$

where Q_0 = primary concentrations of drugs and K_1 = Rate constant for First order.

$$\text{Higuchi model } Q = K_0 t^{1/2} \dots \quad (\text{iii})$$

The various kinetic models were carried out using the mathematical equations, where the data show good linearity for Higuchi, korsmeyer-peppas, zero order and first order models with R^2 value 0.9859, 0.9330, 0.9223 and 0.7575 respectively, where AIC (Akaike Information Criteria) values

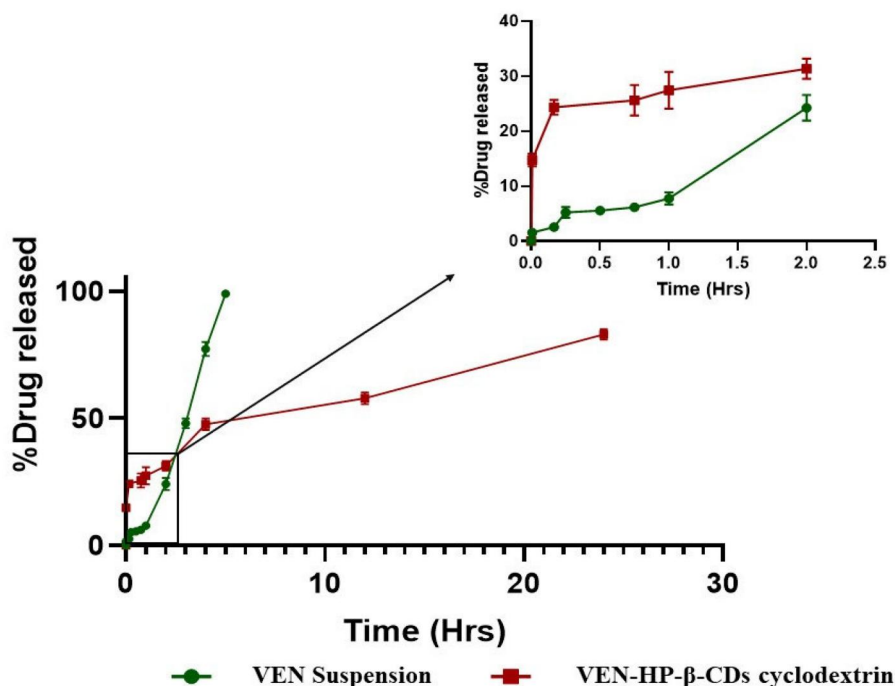


Figure 9. Schematic representation of in-vitro drug releases of VEN from VEN suspension and VEN-HP- β -CDs cyclodextrin formulation. Data were constituted as mean \pm SD ($n = 3$).

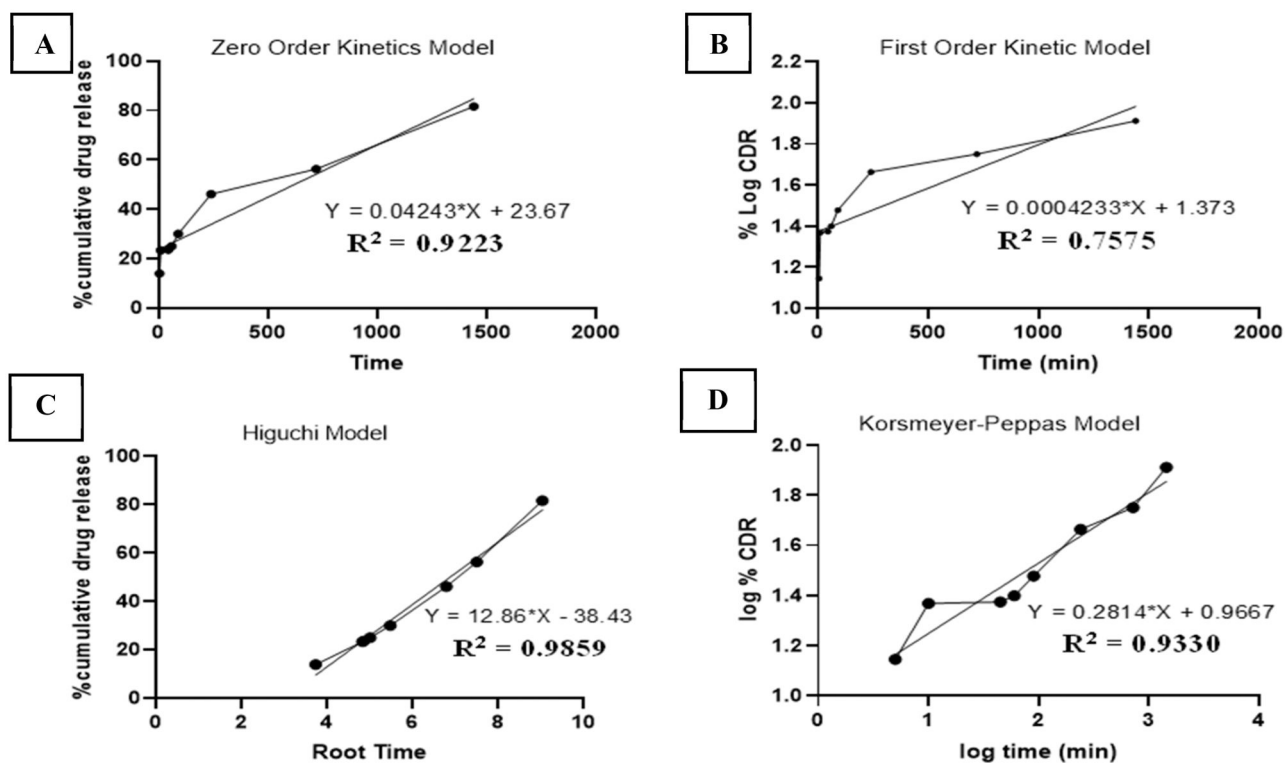


Figure 10. The drug release kinetic models A) Zero order kinetic, B) First order kinetics, C) Higuchi model, D) Korsmeyer-Peppas model for cyclodextrin formulation.

were observed to be 84.31, 122.26, 90.97, and 114.92. Upon considering the high R^2 and Low AIC values Higuchi model was suggested by DD solver programmer, which indicates the diffusion mechanism of drug from cyclodextrin complex as shown in Figure 10. The release exponent was found to be 12.86 for VEN loaded cyclodextrin formulation thus, it ultimately indicates non-Fickian diffusion as exponent is not

less than 0.45. The release pattern of drug in this formulation is likely attributed to the interaction between the drug and HP- β -CD complex. In this scenario, the concentration gradient plays a significant role in governing the release of the drug from the matrix. Specifically, as the drug is dissolved at the matrix surface, a concentration gradient is established. This gradient disparity prompts a diffusion process that

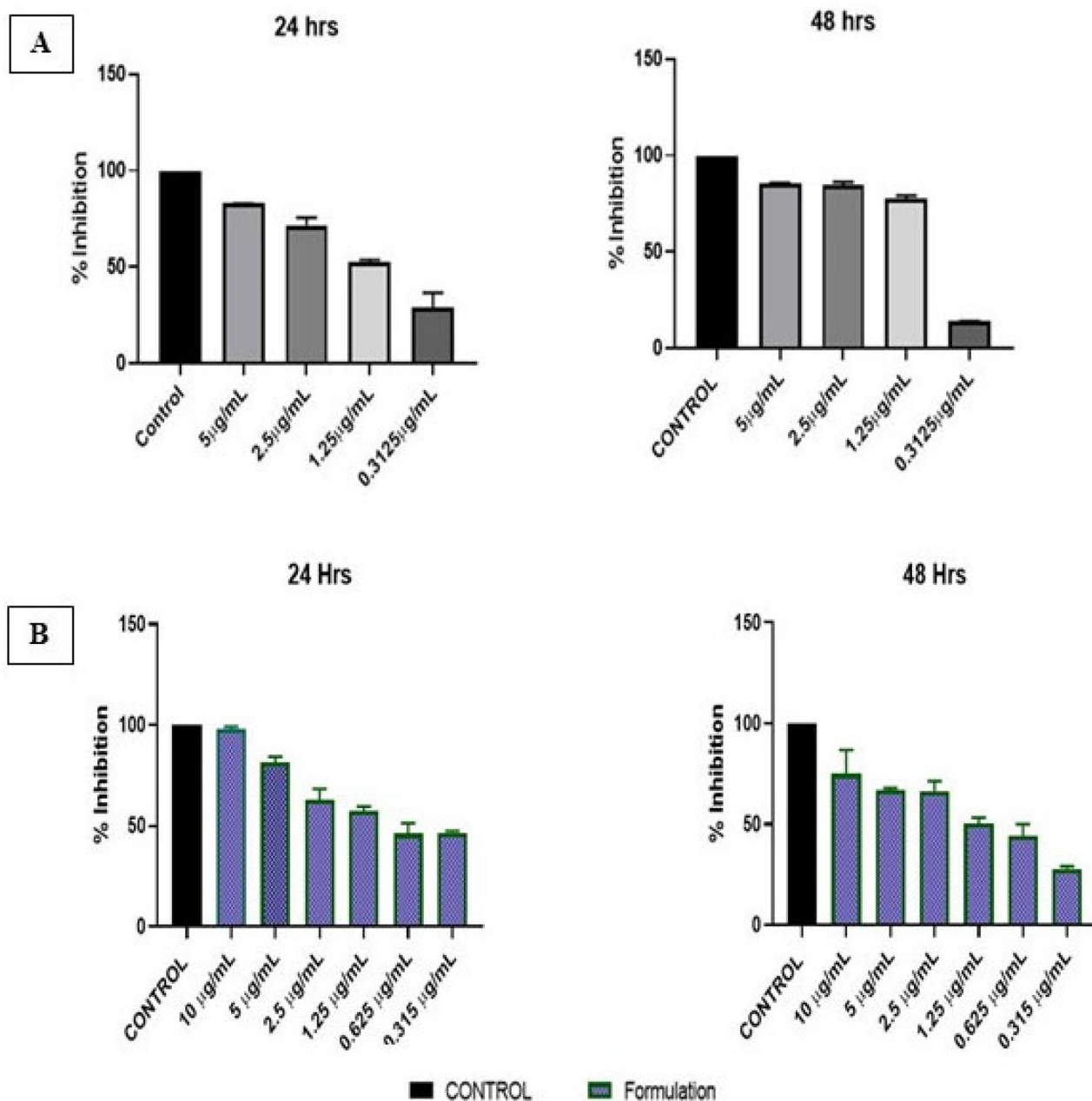


Figure 11. The in-vitro cell cytotoxicity studies were performed on A549 lung cancer cells shows IC₅₀ value of (A) Drug and (B) Formulation at 24, 48 hrs was found as 0.757719, 0.6125 $\mu\text{g/mL}$ as well. Data were constituted as mean \pm SD ($n = 3$).

propels the drug from the inner layers to the outer layers. The release mechanism can be described as diffusion-controlled, as per the principles outlined in the Higuchi equation.

3.8. Cell cytotoxicity data

Figure 11 illustrates the *in-vitro* cytotoxicity data of the Venetoclax and cyclodextrin complex at both 24 hrs and 48 hrs. The IC₅₀ values were found for Venetoclax (1.24 $\mu\text{g/mL}$ and 0.68 $\mu\text{g/mL}$) as well as for cyclodextrin formulation (0.757719 and 0.6125 $\mu\text{g/mL}$) at 24 and 48 hrs, respectively. The data shows IC₅₀ value of cyclodextrin complex was 1.64 folds lesser than pure drug in A-549 cell lines at 24 hrs and

1.12 folds in 48 hrs time interval. Where the pure Venetoclax shows less toxicity to the cancer cells due to the formation of reactive oxygen species, thus enhancing the cell death with respective to the concentration. So far, this is a debut study report on the development and characterization of the venetoclax–cyclodextrin inclusion complexes for the effective management of the lung cancer.

3.9. Qualitative cell apoptosis assay

DAPI is a blue fluorescent dye that is employed to label the nucleus of cells. Staining the nucleus with DAPI is advantageous, as it allows clear differentiation of apoptotic cells through nuclear changes like condensed or fragmented

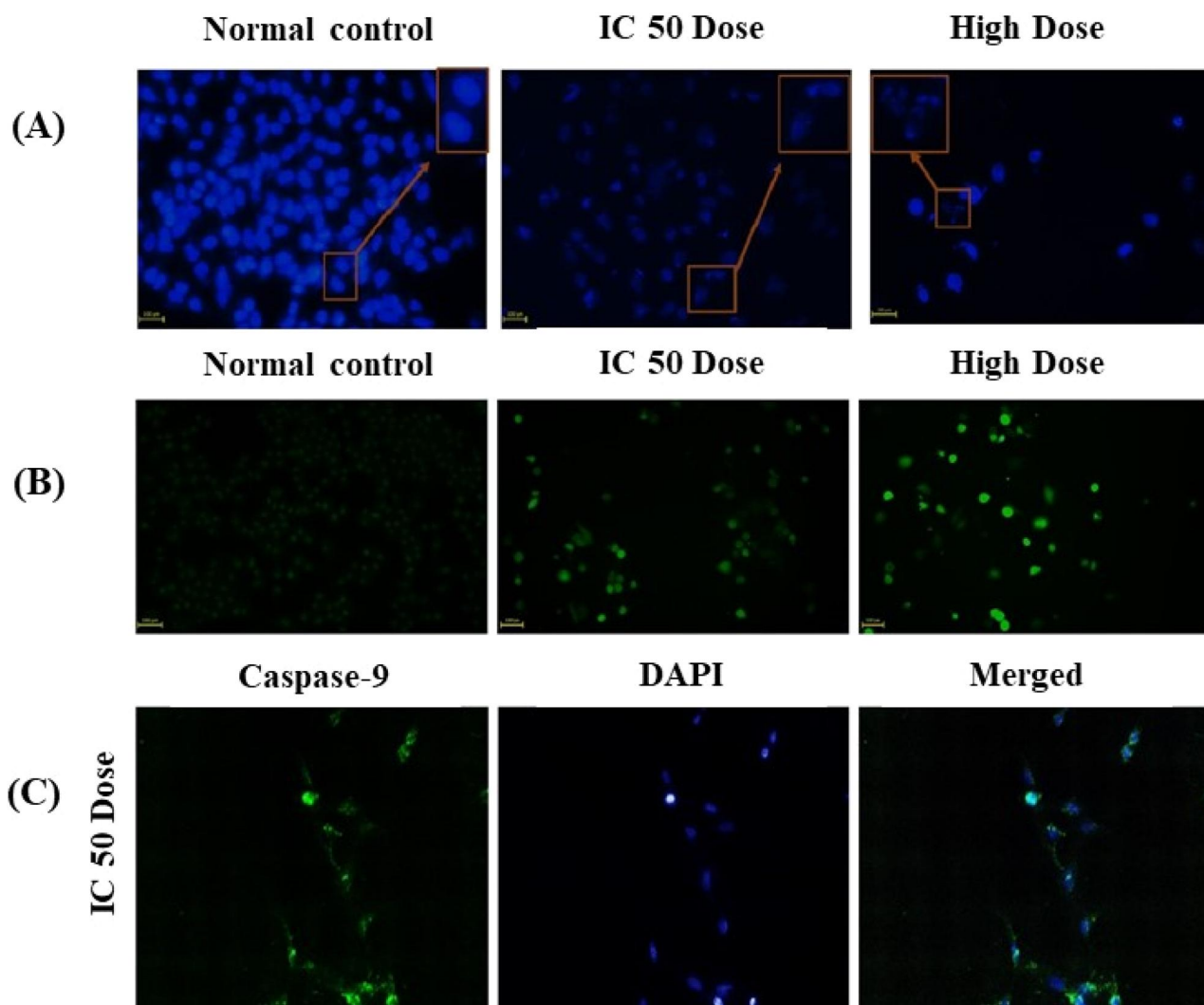


Figure 12. (A) Presents DAPI staining images, which depict morphological changes in the Normal control group of A-549 cells following treatment with the IC50 dose and high dose of formulation over a 24-hrs period. Additionally, (B) shows DCFDA staining of the Normal control group of A-549 cells following treatment with the IC50 dose and high dose of drug-loaded formulation for 24 hrs. Lastly, (C) involved an immunofluorescence assay that aimed to establish the expression of caspase 9 activity within the IC50 dose-treated group of A-549 cell lines.

chromatin, bright nuclei, and horseshoe-shaped nuclei. This labeling technique provides a clear indication of the morphological changes that occur during apoptosis, making it an essential tool in the field of cell biology. Figure 12(A) shows DAPI nucleic acid staining was employed to investigate A-549 cells that had been treated with a drug-loaded formulation. Following the treatment, the A-549 cells displayed significant nuclear alterations like condensed and bright nuclei. These changes indicate the occurrence of apoptosis, which is a programmed cell death mechanism that plays a crucial role in several physiological processes. These morphological changes are often observed in apoptotic cells, making them a reliable indicator of cellular apoptosis. Conversely, in the normal control of the cells, the nucleus remained intact.

3.9.1. DCFDA staining (Reactive Oxygen Species (ROS) generation)

DCFDA (2',7'-dichlorofluorescein diacetate) is utilized for the purpose of detecting Reactive Oxygen Species (ROS) that have been generated within cells. Anti-cancer agents are

capable of producing ROS, which can result in the damage of cell membranes, nucleic acids, proteins, cell organelles, and structural lipids. The end result of this damage is apoptosis, a process in which ROS plays a significant role in cellular disruption and immune system function. As seen in Figure 12(B), DCFDA staining was employed, and the results indicated that the generation of ROS was observed in A-549 cells that had been treated with the drug-loaded formulation, as opposed to normal cells.

3.9.2. Immunofluorescence assay

To identify protein expression in apoptotic cells, the immunofluorescence assay is utilized, with caspase-9 protein being a significant marker in such cells. Figure 12(C) illustrates the detection of caspase-9, DAPI, and merged channels, which display the intensity of the pro-apoptotic marker caspase-9 following treatment with the IC50 dose, along with changes in the cell structure as observed by DAPI stains. The merged images depict the expression of the pro-apoptotic marker in A-549 cells, leading to the inhibition of the

Table 2. Comparative pharmacokinetic parameters of VEN-HP-B-CD and VEN-suspension after oral administration in rat model.

Pharmacokinetic parameters	VEN-HP-B-CD	VEN-suspension
$t_{1/2}$ (min)	803.91	1264.82
T_{max} (min)	120	360
C_{max} ($\mu\text{g/ml}$)	0.85	0.075
AUC_{0-t} ($\mu\text{g/ml}\cdot\text{min}$)	285.13	70.67
$AUC_{0-\infty}$ ($\mu\text{g/ml}\cdot\text{min}$)	342.47	135.77
$AUMC_{0-\infty}$ ($\mu\text{g/ml}\cdot\text{min}^2$)	259217.01	259349.96
$MRT_{0-\infty}$ (min)	756.90	1910.15
V_d [(mg)/($\mu\text{g/ml}$)]	84.66	335.99
Cl [(mg)/($\mu\text{g/ml}$)/min]	0.072	0.18

BCL-2 receptor. The BCL-2 receptor apoptosis pathway results in the generation and enhancement of pro-apoptotic markers such as caspase 3/7/9 while reducing anti-apoptotic markers such as BCL-2 proteins. In this study, the fluorescence intensity of caspase-9 was significantly increased in the treated groups of A-549 cells. Thus, the immunofluorescence assay confirms that the drug-loaded formulation inhibits the BCL-2 receptor, leading to increased pro-apoptotic activity of caspase-9 protein in A-549 cells.

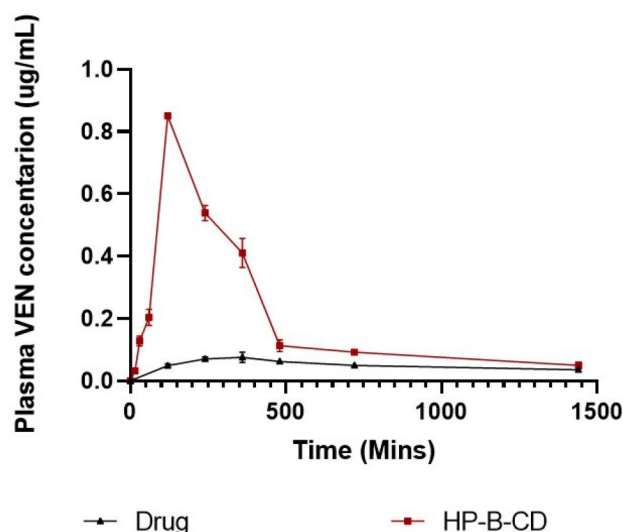
3.10. In-vivo pharmacokinetic studies

In order to improve the oral bioavailability of VEN, researchers developed a complex of VEN-loaded HP- β -CDs. The plasma concentration of VEN released from this complex were compared to pure VEN suspension containing 0.5% tween 80. PK parameters were calculated using PK solver 2.0 represented in Table 2. The plasma-drug concentration time curves are depicted in Figure 13. The study results revealed that the maximum plasma concentration (C_{max}) of VEN from VEN- HP- β -CD was 0.8501 $\mu\text{g/ml}$, which was 11.31 times higher than the C_{max} of 0.07512 $\mu\text{g/ml}$ for VEN suspension. This suggests that the cyclo-dextrin complex formulation enhanced the oral absorption of VEN. Furthermore, the AUC_{0-24} and $AUC_{0-\infty}$ of VEN- HP- β -CD were 4.03 and 2.52 times higher, respectively, compared to those of the VEN suspension. The $t_{1/2}$ for the VEN group was greater than that of the VEN- HP- β -CD group, indicating that the complex formulation had better absorption than the free drug group. The increased absorption of VEN after oral administration may be due to increased dissociation rate and solubility resulting from complexation with HP- β -CDs. The T_{max} of VEN-HP- β -CD group was shorter than that for the VEN group, which was consistent with the $T_{1/2}$ obtained. The oral bioavailability was increased 4.03 times compared to the pure drug.

The study performed a statistical analysis of the pharmacokinetic parameters using a non-parametric unpaired t-test. The results of the analysis revealed that the mean C_{max} ($p < 0.005$) and AUC_{0-24} , $AUC_{0-\infty}$ ($p < 0.05$) of VEN- HP- β -CD were significantly higher than those of the pure VEN suspension. This confirms the improved oral bioavailability of VEN with the use of the HP- β -CD complex.

4. Conclusion

In formulating inclusion complexes with HP- β -CD for the poorly water-soluble Venetoclax, a significant improvement in aqueous solubility and anticancer therapeutic activity on A-549 cancer

**Figure 13.** Plasma concentration in wistar rat administered with Venetoclax and VEN-HP- β -CD Complex.

cells. Stoichiometric ratios were determined through phase solubility studies, and the kneading method emerged as the most suitable for VEN- inclusion complex formulation, overcoming challenges such as contamination, lower yield of product, non-uniformity and stickiness nature. From the preliminary studies like molecular docking and NMR analysis, it was identified that the guest molecule is well encapsulated into the host molecule and confirmed through the physicochemical characterization. Entrapment efficiency and drug loading capacity of this inclusion complex was observed to be $95.44 \pm 0.3\%$ and $33.33 \pm 0.2\%$, respectively. The solubility was enhanced up-to 3.16 ± 0.2 folds as compared to pure drug suspension and improved solubility and dissolution profiles of Venetoclax may lead to enhanced pharmacokinetic parameters of Venetoclax in pre-clinical and clinical studies. The drug release studies for the formulation were observed to be 81.65% in 24 hrs and the application of Higuchi model yielded an R^2 value of 0.9859. The cell cytotoxicity assay proves that IC_{50} value of cyclodextrin inclusion complex are lesser than that of pure drug. Nuclear changes such as condensed and bright nuclei were observed in A-549 cells upon treatment with formulation using DAPI. The overexpression of caspase-9 activity in an apoptotic cell was determined using an immunofluorescence assay. The VEN- HP- β -CD group exhibited a shorter T_{max} compared to the VEN group, in line with the obtained $T_{1/2}$. DCFDA staining shows the generation of ROS was observed in the formulation treated A 549 cells compared to normal cells. The oral bioavailability was increased 4.03 times compared to the pure drug. Thus, prepared formulation suggests that it is a suitable formulation helps in cure of lungs cancers. Furthermore, studies were involved to expose on in-vivo appraisal of cyclodextrins formulation for the conduction of pharmacodynamics studies.

Acknowledgements

We acknowledge to the Department of Pharmaceuticals, National Institute of Pharmaceutical Education and Research NIPER Hyderabad, Ministry of Chemicals and Fertilizers, New Delhi.

Disclosure statement

No potential conflict of interest was reported by the authors.

Funding

The authors reported there is no funding associated with the work featured in this article.

References

- Abarca, R. L., Rodríguez, F. J., Guarda, A., Galotto, M. J., & Bruna, J. E. (2016). Characterization of beta-cyclodextrin inclusion complexes containing an essential oil component. *Food Chemistry*, *196*, 968–975. <https://doi.org/10.1016/j.foodchem.2015.10.023>
- Al-Abboodi, A. S., Al-Sheikh, M., Eid, E. E. M., Azam, F., & Al-Qubaisi, M. S. (2021). Inclusion complex of clausenidin with hydroxypropyl- β -cyclodextrin: Improved physicochemical properties and anti-colon cancer activity. *Saudi Pharmaceutical Journal: SPJ: The Official Publication of the Saudi Pharmaceutical Society*, *29*(3), 223–235. <https://doi.org/10.1016/j.jsps.2021.01.006>
- Alhoshani, A., Alatawi, F. O., Al-Anazi, F. E., Attafi, I. M., Zeidan, A., Agouni, A., El Gamal, H. M., Shamoan, L. S., Khalaf, S., & Korashy, H. M. (2020). BCL-2 inhibitor venetoclax induces autophagy-associated cell death, cell cycle arrest, and apoptosis in human breast cancer cells. *OncoTargets and Therapy*, *13*, 13357–13370. <https://doi.org/10.2147/OTT.S281519>
- Anderson, M. A., Deng, J., Seymour, J. F., Tam, C., Kim, S. Y., Fein, J., Yu, L., Brown, J. R., Westerman, D., Si, E. G., Majewski, I. J., Segal, D., Enschede, S. L. H., Huang, D. C. S., Davids, M. S., Letai, A., & Roberts, A. W. (2016). The BCL2 selective inhibitor venetoclax induces rapid onset apoptosis of CLL cells in patients via a TP53-independent mechanism. *Blood*, *127*(25), 3215–3224. <https://doi.org/10.1182/blood-2016-01-688796>
- Avgerinos, K. I., Spyrou, N., Mantzoros, C. S., & Dalamaga, M. (2019). Obesity and cancer risk: Emerging biological mechanisms and perspectives. *Metabolism: Clinical and Experimental*, *92*, 121–135. <https://doi.org/10.1016/j.metabol.2018.11.001>
- Bhalani, D. V., Bhangaradiya, N., Kumar, A., & Chandel, A. K. S. (2022). Bioavailability enhancement techniques for poorly aqueous soluble drugs and therapeutics. *Biomedicines*, 1–42. <https://doi.org/10.20944/preprints202208.0021.v1>
- Cabral, H. M., & Hadgraft, J. (1990). Studies of cyclodextrin inclusion complexes. I. The Salbutamol-Cyclodextrin Complex as Studied by Phase Solubility and -DSC. *International Journal of Pharmaceutics*, *63*, 259–266.
- Charumane, S., Okonogi, S., Sirithunyalug, J., Wolschann, P., & Viernstein, H. (2016). Effect of cyclodextrin types and co-solvent on solubility of a poorly water soluble drug. *Scientia Pharmaceutica*, *84*(4), 694–704. <https://doi.org/10.3390/scipharm84040694>
- Chary, P. S., Rajana, N., Devabattula, G., Bhavana, V., Singh, H., Godugu, C., Guru, S. K., Singh, S. B., & Mehra, N. K. (2022). Design, fabrication and evaluation of stabilized polymeric mixed micelles for effective management in cancer therapy. *Pharmaceutical Research*, *39*(11), 2761–2780. <https://doi.org/10.1007/S11095-022-03395-8/METRICS>
- Chaudhary, V. B., & Pharmacy, S. S. (2013). Cyclodextrin inclusion complex to enhance solubility of poorly water soluble drugs: A review. *International Journal of Pharmaceutical Sciences and Research*, *4*(1), 68–76.
- de Miranda, J. C., Martins, T. E. A., Veiga, F., & Ferraz, H. G. (2011). Cyclodextrins and ternary complexes: Technology to improve solubility of poorly soluble drugs. *Brazilian Journal of Pharmaceutical Sciences*, *47*(4), 665–681. <https://doi.org/10.1590/S1984-82502011000400003>
- Deeks, E. D. (2016). Venetoclax: First global approval. *Drugs*, *76*(9), 979–987. <https://doi.org/10.1007/s40265-016-0596-x>
- Fang, S., Peng, X., Liang, X., Shen, J., Wang, J., Chen, J., & Meng, Y. (2020). Enhancing water solubility and stability of natamycin by molecular encapsulation in methyl- β -cyclodextrin and its mechanisms by molecular dynamics simulations. *Food Biophysics*, *15*(2), 188–195. <https://doi.org/10.1007/S11483-019-09620-Z/METRICS>
- Ferlay, J., Parkin, D. M., Colombet, M., Soerjomataram, I., Piñeros, M., Znaor, A., & Bray, F. (2021). Cancer statistics for the year 2020: An overview. *International Journal of Cancer*, *149*(4), 778–789. <https://doi.org/10.1002/ijc.33588>
- Gao, S., Liu, Y., Jiang, J., Ji, Q., Fu, Y., Zhao, L., Li, C., & Ye, F. (2019). Physicochemical properties and fungicidal activity of inclusion complexes of fungicide chlorothalonil with β -cyclodextrin and hydroxypropyl- β -cyclodextrin. *Journal of Molecular Liquids*, *293*, 111513. <https://doi.org/10.1016/j.molliq.2019.111513>
- Garnero, C., Aiassa, V., & Longhi, M. (2012). Sulfamethoxazole: hydroxypropyl- β -cyclodextrin complex: Preparation and characterization. *Journal of Pharmaceutical and Biomedical Analysis*, *63*, 74–79. <https://doi.org/10.1016/j.jpba.2012.01.011>
- Garnero, C., Karina, A., & Longhi, M. (2014). Improving furosemide polymorphs properties through supramolecular complexes of β -cyclodextrin. *Journal of Pharmaceutical and Biomedical Analysis*, *95*, 139–145. <https://doi.org/10.1016/j.jpba.2014.02.017>
- Goh, S. Q., Adnan, R., & Rahim, N. Y. (2022). Mini review on synthesis and characterization methods for ternary inclusion complexes of cyclodextrins with drugs. *Malaysian Journal of Chemistry*, *24*(1), 54–72. <https://doi.org/10.55373/mjchem.v24i1>
- Haimhoffer, Á., Rusznyák, Á., Réti-Nagy, K., Vasvári, G., Váradi, J., Vecsernyés, M., Bácskay, I., Fehér, P., Ujhelyi, Z., & Fenyvesi, F. (2019). Cyclodextrins in drug delivery systems and their effects on biological barriers. *Scientia Pharmaceutica*, *87*(4), 33. <https://doi.org/10.3390/scipharm87040033>
- Hidau, M. K., Mehra, N. K., Kolluru, S., & Palakurthi, S. (2017). Cyclodextrin complexation of meclizine hydrochloride and its influence on the solubility for its repurposing. *Drug Delivery Letters*, *7*(1), 54–61. <https://doi.org/10.2174/22103031076661702151306>
- Lodagekar, A., Borkar, R. M., Thatikonda, S., Chavan, R. B., Naidu, V. G. M., Shastri, N. R., Srinivas, R., & Chella, N. (2019). Formulation and evaluation of cyclodextrin complexes for improved anticancer activity of repurposed drug: Niclosamide. *Carbohydrate Polymers*, *212*(January), 252–259. <https://doi.org/10.1016/j.carbpol.2019.02.041>
- Loftsson, T., Jarho, P., Másson, M., & Järvinen, T. (2005). Cyclodextrins in drug delivery. *Expert Opinion on Drug Delivery*, *2*(2), 335–351. <https://doi.org/10.1517/17425247.2.1.335> <https://doi.org/10.1517/17425247.2.1.335>
- Mallardo, S., De Vito, V., Malinconico, M., Volpe, M. G., Santagata, G., & Di Lorenzo, M. L. (2016). Poly(butylene succinate)-based composites containing β -cyclodextrin/d-limonene inclusion complex. *European Polymer Journal*, *79*, 82–96. <https://doi.org/10.1016/j.eurpolymj.2016.04.024>
- Mehra, N. K., Mishra, V., & Jain, N. K. (2013). Receptor-based targeting of therapeutics. *Therapeutic Delivery*, *4*(3), 369–394. <https://doi.org/10.4155/TDE.13.6> <https://doi.org/10.4155/Tde.13.6>
- Mehra, N. K., Verma, A. K., Mishra, P. R., & Jain, N. K. (2014). The cancer targeting potential of d- α -tocopheryl polyethylene glycol 1000 succinate tethered multi walled carbon nanotubes. *Biomaterials*, *35*(15), 4573–4588. <https://doi.org/10.1016/J.BIOMATERIALS.2014.02.022>
- Palakurthi, S., Kolluru, S., Mehra, N., & Hidau, M. (2017). Cyclodextrin complexation of meclizine hydrochloride and its influence on the solubility for its repurposing. *Drug Delivery Letters*, *7*(1), 54–61. <https://doi.org/10.2174/2210303107666170215130631>
- Pavlidis, N., Briasoulis, E., Hainsworth, J., & Greco, F. A. (2005). Diagnostic and therapeutic management of cancer of an unknown primary. *European Journal of Cancer (Oxford, England: 1990)*, *39*(14), 1990–2005. [https://doi.org/10.1016/S0959-8049\(03\)00547-1](https://doi.org/10.1016/S0959-8049(03)00547-1)
- Pereira, A. G., Carpena, M., Oliveira, P. G., Mejuto, J. C., Prieto, M. A., & Gandara, J. S. (2021). Main applications of cyclodextrins in the food industry as the compounds of choice to form host-guest complexes. *International Journal of Molecular Sciences*, *22*(3), 1–23. <https://doi.org/10.3390/ijms22031339>
- Rudrangi, S. R. S., Bhomia, R., Trivedi, V., Vine, G. J., Mitchell, J. C., Alexander, B. D., & Wicks, S. R. (2015). Influence of the preparation method on the physicochemical properties of indomethacin and methyl- β -cyclodextrin complexes. *International Journal of Pharmaceutics*, *479*(2), 381–390. <https://doi.org/10.1016/J.IJPHARM.2015.01.010>

- Salih, M., Omolo, C. A., Agrawal, N., Walvekar, P., Waddad, A. Y., Mocktar, C., Ramdhan, C., & Govender, T. (2019). Supramolecular amphiphiles of beta-cyclodextrin and oleylamine for enhancement of vancomycin delivery. *International Journal of Pharmaceutics*, 574, 118881. <https://doi.org/10.1016/j.ijpharm.2019.118881>
- Sambasevam, K. P., Mohamad, S., Sarih, N. M., & Ismail, N. A. (2013). Synthesis and characterization of the inclusion complex of β -cyclodextrin and Azomethine. *International Journal of Molecular Sciences*, 14(2), 3671–3682. <https://doi.org/10.3390/ijms14023671>
- Shukla, S. K., Chan, A., Parvathaneni, V., Kanabar, D. D., Patel, K., Ayehunie, S., Muth, A., & Gupta, V. (2020). Enhanced solubility, stability, permeation and anti-cancer efficacy of Celestrol- β -cyclodextrin inclusion complex. *Journal of Molecular Liquids*, 318, 113936. <https://doi.org/10.1016/j.molliq.2020.113936>
- Suvarna, V., Kajwe, A., Murahari, M., Pujar, G. V., Inturi, B. K., & Sherje, A. P. (2017). Inclusion complexes of nateglinide with HP- β -CD and L-arginine for solubility and dissolution enhancement: Preparation, characterization, and molecular docking study. *Journal of Pharmaceutical Innovation*, 12(2), 168–181. <https://doi.org/10.1007/s12247-017-9275-z>
- Torres-Alvarez, C., Castillo, S., Sánchez-García, E., González, C. A., Galindo-Rodríguez, S. A., Gabaldón-Hernández, J. A., & Báez-González, J. G. (2020). Inclusion complexes of concentrated orange oils and β -cyclodextrin : Physicochemical and biological characterizations. *Molecules (Basel, Switzerland)*, 25(21), 5109. <https://doi.org/10.3390/molecules25215109>
- Vaidya, B., Shukla, S. K., Kolluru, S., Huen, M., Mulla, N., Mehra, N., Kanabar, D., Palakurthi, S., Ayehunie, S., Muth, A., & Gupta, V. (2019). Nintedanib-cyclodextrin complex to improve bio-activity and intestinal permeability. *Carbohydrate Polymers*, 204, 68–77. <https://doi.org/10.1016/J.CARBPOL.2018.09.080>
- Yang, G., Chen, W., & Ho, E. H. L. (2002). Design and kinematic analysis of a modular hybrid parallel-serial manipulator. *Proceedings of the 7th International Conference on Control, Automation, Robotics and Vision, ICARCV 2002*, 45–50. <https://doi.org/10.1109/ICARCV.2002.1234788>